Lithos xxx (2015) xxx–xxx

Contents lists available at ScienceDirect

Lithos

journal homepage: www.elsevier.com/locate/lithos

Synthesis paper

Platinum group elements in mantle melts and mantle samples

Stephen J. Barnes [a],*, James E. Mungall [b], Wolfgang D. Maier [c]

[a] Mineral Resources Flagship, CSIRO, Perth, Western Australia, Australia
[b] Department of Earth Sciences, University of Toronto, Canada
[c] School of Earth and Ocean Sciences, Cardiff University, UK

ARTICLE INFO

Article history:
Received 19 December 2014
Accepted 2 July 2015
Available online xxxx

Keywords:
Partial melting
Lithosphere
Large igneous province
Komatiite
Basalt
Sampling

ABSTRACT

A large data compilation has been assembled of platinum group element (PGE) analyses in mantle melts and mantle rocks, the latter including an assortment of xenoliths and obducted mantle massifs. The degree of correlation has been investigated among the PGEs and with other major element variables such as Al_2O_3, TiO_2 and Mg number, and the results are considered in the context of the current paradigm for the behaviour of highly siderophile elements in the silicate Earth.

Primitive mantle melts have a wide range of PGE contents. Komatiites have the highest abundances of all the PGEs, show the strongest correlations between Pt and Rh, Pt and Pd and between the iridium-group PGEs Ir, Ru and Os (IPGEs). Most basalts of all affinities have lower levels of Pt and Pd and much lower levels of Ir, Ru and Os than komatiites. Within the basalt grouping Rh has stronger affinities with the IPGEs. Picrites and Archaean basalts are intermediate between these two groups. MORBs and a small proportion of continental LIP basalts show strong depletions in all PGEs attributable to retention of sulfide in their mantle source rocks, or sulfide liquid fractionation on ascent. The degree of PGE depletion in other basalts is probably attributable to equilibration with sulfide, but is less than would be expected under conventional models of sulfide extraction, and is instead attributed to mixing of magmas generated at variable depths incorporating both sulfide-saturated and undersaturated components. Basalts with Pt and Pd contents higher than typical komatiites are rare, a notable example being B1-type parent magmas to the Bushveld Complex, which have komatiite-like relative PGE abundances and Pt, Pd and Rh abundances up to a factor of two higher than komatiites for comparable Ti contents.

The mantle composition array as a whole is characterized by variable degrees of depletion of Pt, Pd and Rh in Al-poor, melt-depleted harzburgite/dunite lithologies; lack of depletion in these elements in Al-bearing lherzolites; and a lack of systematic variation in IPGEs across this range. Strongest correlations across the entire set are observed between Ir, Ru and Os; and between Pt and Rh. Melt-depleted cratonic mantle samples are notably more deficient in Pd than in Pt, but comparable Pd-enriched components are not represented in the available data from continental environments. The only group of mantle melts that systematically record high Pd/Pt ratios are MORBs; if these are indeed the complement of the depleted cratonic mantle suite then the melt depletion recorded by the cratonic mantle suite occurred at low pressure prior to tectonic underplating of the depleted lithosphere beneath the cratons. A filtered subset of orogenic peridotite compositions that are thought not to have been affected by significant extents of melt extraction or metasomatic refertilization have median concentrations of 3.9 ppb Os, 2.9 ppb Ir, 6.3 ppb Ru, 1.0 ppb Rh, 6.2 ppb Pt, 5.4 ppb Pd, and Cu/Pd ratio of 5500, which we consider to be representative of the modern convecting mantle. The convecting mantle has PGE proportions closely resembling those of lunar impact breccias, diverging considerably from chondritic proportions and attributable to the presence of a late veneer-derived, predominantly sulfide-hosted component. The compositions of mantle peridotites show considerable scatter attributable to the combined effects of measurement error and a strong covariance due to a heterogeneous distribution of sulfide in the small samples typically chosen for pulverization. The intensity of the covariance between all of the PGE due to sampling error gives a false impression of a genetic trend toward highly enriched PGE in some samples which could be mistaken for the effects of metasomatism; however no plausible metasomatic process would be expected to retain the tight interelement correlations shown.

1. Introduction

The platinum group elements (PGEs) – Pt, Pd, Rh, Ru, Ir and Os – are informative tracers of a wide variety of petrogenetic processes including

---

* Corresponding author.
E-mail address: steve.barnes@csiro.au (S.J. Barnes).

http://dx.doi.org/10.1016/j.lithos.2015.07.007
0024-4937/© 2015 Elsevier B.V. All rights reserved.

Please cite this article as: Barnes, S.J., et al., Platinum group elements in mantle melts and mantle samples, Lithos (2015), http://dx.doi.org/10.1016/j.lithos.2015.07.007

planetary accretion and differentiation (Lorand et al., 2008b), core formation (Gaetani and Grove, 1997; Murthy and Karato, 1997), late-veneer addition and homogenization (Chou, 1978; Maier et al., 2009; Morgan et al., 2001), depletion and fertilization of continental lithosphere (Becker et al., 2006; Lorand et al., 2010, 2012; Maier et al., 2012a), timing of sulfide saturation in mafic and ultramafic magmas and genesis of magmatic sulfide ores (Barnes et al., 1985; Hamlyn and Keays, 1986; Keays, 1995). The latter application has found practical applications in exploration for magmatic sulfide orebodies (Barnes et al., 2013; Fiorentini et al., 2010; Lesher et al., 2001; Maier and Barnes, 1999). Understanding the geochemistry of the PGEs has become particularly important in view of the now widespread use of the Re–Os isotopic system to date major processes of planetary differentiation, the age of the subcontinental lithosphere and the timing of formation of the continents themselves (Griffin et al., 2004; Shirey and Walker, 1998).

A large body of high quality data has accumulated in the last two or three decades, following the development of a variety of extremely sensitive and precise analytical techniques. The PGEs and Re are among the least abundant elements not only in the crust but in the silicate portion of the Earth as a whole (McDonough and Sun, 1995), and they are the only suite of elements in the periodic table (along with Au) whose abundances are routinely analysed in silicate rocks at low-ppb or even sub-ppb levels.

The igneous geochemical behaviour of this complex suite of elements is especially complex, owing to the tendency of PGE behaviour to be controlled by the stability of accessory, trace and ultra-trace phases during magmatic processes. Previous reviews have considered large datasets for magmas on the one hand (Barnes and Fiorentini, 2008; Day et al., 2013; Fiorentini et al., 2010) and for mantle samples on the other (Lorand et al., 2012), but taking a broad overview of these datasets in combination offers an opportunity to pick out essential relationships, especially when combined with some of the recent insights derived from new micro-analytical techniques (Alard et al., 2000), and from many decades of study of the distribution of PGEs in magmatic ore deposits, summarized in reviews by Naldrett (2004), and Barnes and Lightfoot (2005). This contribution attempts to use a combination of data on PGEs in samples of mantle melts and mantle rocks, filtered to remove as far as possible effects of low temperature fractionation and late S saturation.

A major objective of the paper is to make available a comprehensive compilation of data from the literature, subdivided by tectonic setting and rock type. To this end, an extensive set of supplementary data includes complete data listings, sources, and contoured data density plots intended to form a basis for comparison in future PGE studies.

This contribution sets out the data, presents a review of current models for magmatic PGE behaviour, and sets the scene for a companion paper (Mungall and Barnes, in prep) that presents detailed quantitative modelling of mantle melting processes based on the most recent available experimental constraints. We use the data set here to consider some specific current questions in PGE geochemistry, principally:

1) What is the range of variability in PGE contents of relatively unfractionated mantle melts and the sources from which they derive?
2) To what extent are PGE concentrations in mantle melts and restites explicable by current models, and particularly by magmatic sulfide liquid control?
3) To what extent are the PGE budgets of mantle restites and mantle melts complementary?
4) Are current estimates of primitive mantle PGE concentrations reasonable, and to what extent are they modified and controlled by processes of metasomatism and mantle refertilization?

1.1. PGEs in mantle-related rocks: the “standard model”

Following pioneering work in the 1970s and 1980s on PGEs in magmas and sulfide ore deposits (Barnes, 1985; Crocket, 1979; Keays and Crocket, 1970; Keays and Davidson, 1976), a general consensus has built up around the behaviour of the PGEs in mafic and ultramafic melts. In what will be referred to as the “standard model”, the following principles have been widely considered to be firmly established.

1) The predominant control on the concentrations of PGEs in magmas is interaction with magmatic sulfide liquids. All the PGEs are extremely chalcophile under almost all conditions, and partition coefficients from silicate into sulfide liquids are some of the highest for any elements in nature: estimates range from the order of thousands (Fleet et al., 1991), to millions (Andrews and Brenan, 2002b; Fonseca et al., 2009), with recent experimental data confirming values of the order of 10^5 to 10^6 (Mungall and Brenan, 2014). This feature underpins the high and spectacularly variable concentrations of PGEs in magmatic sulfide accumulations in nature (Campbell and Barnes, 1984), and also the extensive depletion of all the PGEs seen in certain basaltic (and some komatiitic) rocks believed to have interacted with magmatic sulfide liquid (Barnes and Picard, 1993; Brügmann et al., 1993; Fiorentini et al., 2010; Rehkämper et al., 1999).
2) The retention or otherwise of magmatic sulfides during mantle partial melting is a critical control on the PGE contents of the resulting melts. The presence of even tiny amounts of residual sulfide is enough to produce strong PGE depletion in mantle melts that are sulfide saturated at source (Hamlyn and Keays, 1986; Mungall, 2014; Mungall and Brenan, 2014). This gives rise to an “all or nothing” mantle source control — instantaneous primary mantle melts are likely to be either highly depleted in PGEs due to sulfide liquid interaction, or not at all, depending on whether the degree of partial melting is sufficiently high to remove all of the source sulfide by dissolving it in the silicate melt.
3) The PGEs fall into two contrasting geochemical groupings. The Ir-series PGEs, denoted the IPGEs by Barnes et al. (1985), comprising Ir, Ru and Os, behave as a coherent group of compatible elements in igneous processes. They are retained in the mantle during partial melting, they decrease in residual melts during fractional crystallization and they are enriched in ultramafic cumulates, all regardless of presence of sulfides. The PPGEs Pt and Pd have precisely the opposite characteristics in the absence of a magmatic sulfide phase (Barnes et al., 1985).
4) The IPGEs are also distinguished by their tendency to form highly refractory phases of their own, particularly alloys, arsenides and sulfides (laurite) in the case of Ru (e.g. Bai et al., 2000; Barnes et al., 2008; Dare et al., 2010; Distler et al., 1999; Liipo, 1999; Page and Talkington, 1984; Peck and Keays, 1992; Zhou et al., 2000). Only Pt of the remaining PGEs shares this characteristic. Refractory IPGE phases, rather than compatibility in silicate or oxide phases, have been generally considered to be a major cause of the compatible behaviour of the group, although Ru is strongly compatible in chromite under some circumstances (Brenan et al., 2012; Locmelis et al., 2011; Page et al., 2012). Refractory IPGEs and their alteration products are very commonly found in close association with chromite in both mantle and crustal ultramafic cumulates (Arai et al., 1999; Legendre and Auge, 1986; Peck and Keays, 1990; Prichard et al., 1981). Experimental data presented and reviewed by Mungall and Brenan (2014) indicates mild compatibility into olivine; on this basis these authors consider the dominant control on compatible behaviour of IPGE to be their partitioning into olivine and chromite, with a subsidiary but detectable additional signal resulting from the existence of alloys or similar PGM.
5) The PGEs can be fractionated from one other during differentiation or partial melting of sulfide magmas. Typical sulfide magmas, particularly those with high Cu contents and hence large melting ranges, have as their primary liquidus phase the high-T equivalent of pyrrhotite referred to as monosulfide solid solution (MSS) and undergo fractional crystallization of this phase, resulting in enrichment of the residual liquid in Cu. The IPGEs and Rh are all compatible in MSS, with D values typically around 2–10, relative to Pt and Pd which are incompatible

Please cite this article as: Barnes, S.J., et al., Platinum group elements in mantle melts and mantle samples, Lithos (2015), http://dx.doi.org/10.1016/j.lithos.2015.07.007

(Li et al., 1996; Mungall et al., 2005). This process leads to large internal variations in PGE concentration within orebodies.In some cases, such as particular deposits at Sudbury and Noril'sk, orebodies are zoned from IPGE enriched, Cu-poor MSS cumulates to extremely Pt, Pd, Ni, and Cu rich bonanza ore shoots formed from highly enriched residual melt (Huminicki et al., 2005; Mungall, 2007a; Naldrett et al., 1982, 1999).

6) The somewhat neglected "middle" PGE, Rh, has apparently intermediate character between the IPGEs and the pairing of Pt and Pd. Rhodium shares with the IPGEs the property of partitioning into MSS during sulfide fractionation, and closely follows the IPGEs during differentiation of magmatic sulfide ores (Barnes, 2004), but lacks the IPGE tendency to make its own phases as a major component. In other respects, as we see below, it follows Pt and Pd. This intermediate character is potentially highly revealing.

1.2. PGEs in mantle-related rocks: recent developments

In the last few years, a number of advances in analytical and experimental techniques, particularly the development of laser ablation — ICPMS (inductively coupled plasma mass spectrometry) analysis at ppb detection limits, have produced a number of intriguing observations that have both positive and negative implications for the standard model. Concurrently, extremely painstaking and detailed investigation of PGE deportment in mantle samples and in sulfide ores and their host rocks has added new mineralogical insights. In summary, the following refinements or modifications to the standard model have either been made or are currently being hotly debated.

1) PGEs are extremely insoluble in silicate melts under normal mantle redox conditions (Andrews and Brenan, 2002a,2002b; Borisov, 2005; Borisov and Palme, 2000; Brenan and Andrews, 2001; Ertel et al., 1999; O'Neill et al., 1995). Solubility values range from low ppb to several tens of ppb. Controversy continues about the role of S in the melt; results of Mungall and Brenan (2014) confirm that the presence of S in the silicate melt substantially increases PGE metal solubility (Laurenz et al., 2013), but even taking this into account solubility values in the low 10s of ppb range are typical at normal oxygen fugacities. Such low solubilities give rise to stability of IPGE-rich phases, and in some cases Pt-rich phases in equilibrium with magmas (Barnes et al., 2014), and the possibility that such phases crystallize directly from magmas, where not prevented from doing so by prior depletion by sulfide liquid. Extremely low solubilities also imply extremely high activity coefficients for PGEs in silicate melts, which, coupled with evidence for high solubilities in sulfide liquids (Fonseca et al., 2009, 2012) are fully consistent with the higher estimates of 10^5 or 10^6 for partition coefficients for PGEs into sulfide melts (Mungall and Brenan, 2014). Recent experiments and the advent of ultra-sensitive laser ablation data have overcome the widespread problem of presence of PGM micronuggets in experimental charges that gave incorrectly low Ds in early experiments (Mungall and Brenan, 2014). Much of the complexity of PGE geochemistry is a consequence of extreme low solubilities and the resulting kinetics of nucleation of PGE-enriched phases from magmas. An example is the common occurrence of IPGE inclusions within chromite; this may be the result of redox-driven nucleation of these phases (Finnigan et al., 2008) in boundary layers around growing or reacting chromite crystals. Another consequence, of enormous significance for the economic geology of the PGEs, may be the spectacularly high PGE tenors of the very first increment of sulfide liquid to nucleate during sulfide saturation events (Ballhaus and Sylvester, 2000; Barnes, 1993; Godel et al., 2014).
2) A long-standing idea in PGE geochemistry is that PGEs are present in melts as "nanoclusters", possibly in combination with other elements such as S, As, Te and Bi. This concept was originated in the 1980s by workers on magmatic PGE "Reef-style" deposits as found in major layered intrusions such as the Bushveld Complex and the Great Dyke (Ballhaus and Sylvester, 2000; Tredoux et al., 1995; Wilson and Tredoux, 1990), and has only recently found some experimental support in observations on As-bearing sulfide melts (Helmy et al., 2013; Kennedy et al., 2013). However, the strong experimental evidence for fO_2 and fS_2 dependence on the solubility of PGEs implies that PGEs dissolve primarily by forming –O and –S bonds, and the nanocluster concept is unnecessary to explain most of the observed behaviour. Furthermore, the textural evidence is equivocal in support of Helmy's assertion that the Pt–As phases observed in their experimental run products were present at run conditions, and we remain unconvinced that these do not represent quench phases.
3) PGE deportment at ppb levels in sub-continental lithospheric mantle samples is complex, and is held to be influenced by metasomatic processes believed to be related to refertilization of previously depleted mantle harzburgite. The IPGEs are associated with refractory IPGE phases and MSS, commonly found as inclusions in olivine. Platinum and Pd are associated with intergranular Cu-bearing sulfides (Alard et al., 2000; Lorand et al., 2008a, 2010, 2012). The two groupings are considered to have been extensively decoupled during evolution of the lithosphere, possibly as a result of incongruent melting of mantle sulfides (Ballhaus et al., 2006).
4) Platinum and Pd, while typically very strongly correlated with one another, become decoupled in some magmatic settings, particularly in cumulate sequences within certain layered intrusions where Pt/Pd and Pt/S ratios can vary widely and erratically on a scale of metres (Barnes et al., 2004a, 2011; Keays et al., 2012; Maier and Barnes, 1999). Fractionation of Pt from Pd has also been documented during low-pressure fractionation in a number of suites, notably the continental LIP sequences in East Greenland (Momme et al., 2002, 2006), the Deccan Traps (Keays and Lightfoot, 2010), the Siberian Traps (Lightfoot and Keays, 2005), the Newer Volcanic Sequence of SE Australia (Vogel and Keays, 1997) and the Pual Ridge lavas (Park and Campbell, 2013). In all cases, where the fractionating melts follow a sulfide liquid undersaturated path, Pd behaves almost perfectly incompatibly, while Pt shows mildly compatible behaviour, leading to an increase in Pd/Pt with declining MgO and Mg/Fe. As we show below, this trend is not evident in high-MgO melts that have not undergone extensive low-pressure fractionation in the crust. Coupled with some rare occurrences of Pt enrichment in ultramafic rocks with no other associated PGEs (Maier et al., 2015), Pt depletion relative to Pd may be taken as evidence for primary magmatic precipitation of Pt-rich phases, probably Pt–Fe alloy or Pt arsenide. Primary Pt or PtFe precipitation may be the ultimate origin of the Pt placer deposits associated with certain Ural–Alaskan complexes (Garuti et al., 1997; Malitch and Thalhammer, 2002).
5) The "all or nothing" model for retention of PGEs by sulfides during mantle melting does not explain the relatively mild degree of PGE depletion in many basaltic rocks, possibly excepting MORBs. The retention of sulfide liquid in the mantle restite during mantle partial melting is an assumption, and depends on a particular physical model of the process that requires re-examination (Ballhaus et al., 2006). In particular, it is debatable whether tiny ten-micron-scale droplets of sulfide liquid generated during partial melting events could be entrained by the escaping melt, or whether they would be trapped in the partially molten peridotite by capillary forces (Chung and Mungall, 2009).

In addition to these developments, a debate has opened up in the economic geology world over whether certain magmas have a particular propensity to form magmatic sulfide deposits owing to interaction with metasomatically enriched sub-continental lithospheric mantle (Griffin et al., 2013). The debate can be traced back to discussions of characteristics of parent magmas to the Bushveld Complex (Hatton and Sharpe, 1989; Richardson and Shirey, 2008) and was developed to consider a number of large igneous provinces by Zhang et al., (2008).

Please cite this article as: Barnes, S.J., et al., Platinum group elements in mantle melts and mantle samples, Lithos (2015), http://dx.doi.org/10.1016/j.lithos.2015.07.007

On the basis of PGE data, Fiorentini et al. (2010) failed to find any significant evidence for unusually PGE rich magmas within komatiitic and plume-related basaltic suites, and Arndt (2013) has argued against any significant role for the SCLM in magmatic sulfide petrogenesis. On the other hand, Au-, Re- and Pd-rich xenoliths in island arc settings argue for a role of mantle fertilization or moderate degrees of melting under unusually oxidizing conditions in generating precious-metal-rich porphyry systems (McInnes et al., 1999; Mungall, 2002), and magmas produced immediately after removal of sulfide from the source mantle either by second stage melting (e.g., Keays, 1995; Mungall and Brenan, 2014) or at low degrees of melting at high fO_2 (Botcharnikov et al., 2013; Mungall et al., 2006) may have extremely high PGE contents if they fail to pool with lower degree partial melts.

The following two sections examine the available whole-rock analytical datasets for mantle melts and mantle samples, and consider their implications for the "standard model" and its various challenges. Data sources with full references can be found in supplementary materials.

2. PGEs in mantle melts

2.1. Data selection and screening

The data set on PGE in mantle melts compiled for this study is very similar to that employed by Fiorentini et al. (2010) with the addition of a recent data set on parental magmas to the Bushveld Complex (Barnes et al., 2010) and some other recently published data on a number of large igneous provinces (Day et al., 2013; Hughes et al., 2015; Li et al., 2010, 2012; Ma et al., 2013; Qi et al., 2008; Song et al., 2006). (Full data sources are listed in supplementary materials). The criteria for inclusion are that data should have been collected within the last twenty years using high-precision, low level analytical techniques: either Ni sulfide fire assay with ICP-MS, or isotope dilution mass spectrometry with Carius tube dissolution. Comparisons of these two techniques are given in Fiorentini et al. (2010). The published datasets were also required to record MgO, FeO and TiO_2 on the same samples. Data are included from all mafic and ultramafic volcanic rocks considered to be mantle melts. Data from komatiites are restricted to those with less than 30% MgO to minimise inclusion of samples containing high proportions of cumulus olivine, and are also restricted to komatiite formations with no known association with magmatic sulfide ores. The komatiite data set is further restricted by excluding Al-depleted (also known as "Barberton-type) komatiites to exclude processes of anomalously deep melting in the majorite stability field (Arndt et al., 2008), and also restricted to komatiites less than 2.9 Ga old to eliminate the secular variation in older komatiites identified by Maier et al. (2009) and attributed to time-dependent homogenization of the PGE-enriched late veneer into the deep mantle.

As the main purpose of this contribution is to trace mantle processes, the data are further filtered to minimise the inclusion of samples that have undergone extensive low pressure fractional crystallization in the crust. This cannot be done rigorously, but use of the FeO–MgO plot (Fig. 1) (Herzberg et al., 2007) provides a simple graphical technique.

The data array of approximately 1300 points shows a broadly L-shaped trend in Fig. 1, the steep leg being defined by wide variability of FeO at a narrow range of low MgO values. This steep trend is attributed to the fractional crystallization of plagioclase bearing assemblages at low pressures. The samples plotting along this trend, falling above the diagonal dashed line on Fig. 1A, were eliminated from the study set. The remaining horizontal trend is attributed to fractionation of olivine from original primitive mantle melts; there is no way to determine how extensive this fractionation was, or where it took place, or how much is due to variable degrees of partial melting rather than fractional crystallization, but restriction to "olivine-controlled" samples is likely to remove at least some and possibly most of the variation due to low-P processes. Residual variation due to olivine fractionation is minimised in the discussion that follows by considering ratios of PGEs to Ti, an element that is incompatible in olivine and also relatively insensitive to contamination by continental crust (Fiorentini et al., 2010).

Filtering for the effects of alteration was not possible for most of the basaltic data, and we could only rely on the choice of the original authors to see fit to publish them in the first place as an indication of freshness. In the case of the komatiite data set, owing to the dominance of olivine control we were able to apply a Pearce element ratio approach (see Barnes et al., 2004b for details) using Si, Al, Fe and Mg to eliminate samples falling significantly off olivine control lines as being unacceptably metasomatised, before incorporating them into the starting data set.

The bulk of the filtered dataset, comprising 856 data points, is derived from a number of distinct tectonic settings, distinguished by colour on the plots that follow. These are: Archaean greenstone belts, dominated by komatiites and associated basalts; Proterozoic supracrustal belts, also containing komatiites and basalts in addition to picrites; continental large igneous provinces (basalts, picrites); ocean islands (basalts and picrites); mid-ocean ridge basalts (basalts); and a small number of analyses from oceanic and continental arcs. For the purposes of this study, samples were classified on the basis of MgO, TiO_2 and tectonic setting into four major lithological groups: komatiites (MgO 18–30% and $TiO_2 < \sim 1$), picrites ($MgO > 12\%$, $TiO_2 > 1$), and low and high TiO_2 basalts (TiO_2 less than or greater than approximately 1.5, respectively; the exact lines of demarcation are shown in Fig. 1B). The picrite group is extended to include high MgO samples from continental Large Igneous Provinces (LIPs) regardless of their TiO_2 content. Within the picrite set, a large proportion of samples probably owe their high MgO contents to the presence of entrained olivine phenocrysts; this is certainly true for the OIB set, which is dominated by Hawaiian picrites explicitly stated to contain phenocryst olivine (Ireland et al., 2009). We have not attempted to eliminate olivine-phyric samples, as the necessary petrographic data with which to do this is not usually available in published data tables. The Bushveld Sills data set, consisting mainly of chilled margins and pyroxene-phyric rocks from marginal sills to the Complex, is broken out separately. These lithogeochemical subdivisions are not the standard definitions, but are simplified to avoid having an indigestible number of classification groups on the plots.

Some inconsistency is present in the suites of elements analysed for different samples. Isotope dilution methods do not report Rh, which is mono-isotopic, and some fire assay analyses do not report Os owing to volatility of oxidized Os during dissolution. Hence both elements are under-represented in the data set as a whole, but in different samples. This imbalance should be borne in mind, particularly within subsets (such as OIB and MORB) with smaller numbers of samples.

The datasets inevitably contain a small proportion of wildly outlying points; these can be accommodated by plotting the data on log–log plots, but it was found that this approach obscures much interesting detail in the bulk of the dataset. For this reason we have selected axes on the various geochemical plots to include approximately 95% of the data, hence excluding a small proportion of the further outliers. This should be born in mind through the following discussion. Additional plots with axis scales chosen to show 99% of the data are provided in the Supplementary Information, along with data density plots for all of the major sample groupings.

2.2. Variations and inter-element correlations

Variation of all the PGEs with Mg number (Molar MgO / [MgO + FeO]) and between one another is shown in a series of multi-element scatter diagrams (Figs. 2, 3, and 4).

The IPGEs Ir, Ru and Os show closely coherent patterns and broadly positive correlations with Mg#, reflecting their generally compatible character, with highest values in komatiites. Picrite and basalt samples from continental large igneous provinces (CLIPs) and ocean island basalt provinces (OIBs) also show weak positive correlations between

Please cite this article as: Barnes, S.J., et al., Platinum group elements in mantle melts and mantle samples, Lithos (2015), http://dx.doi.org/10.1016/j.lithos.2015.07.007

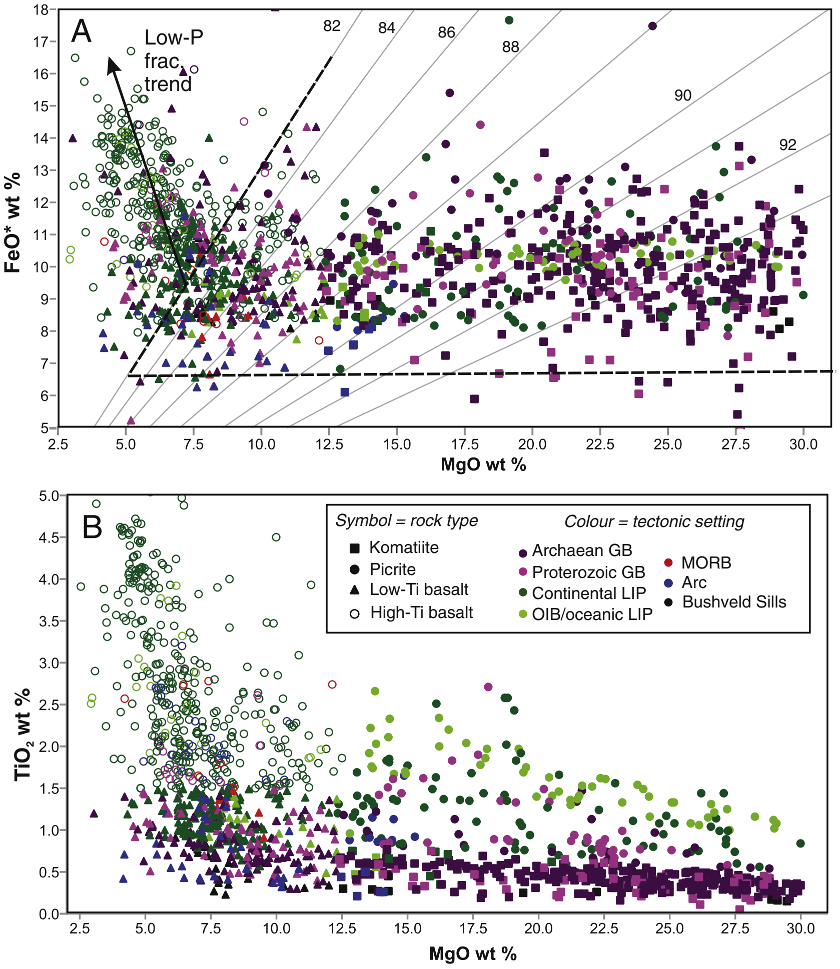

Fig. 1. A. Plot of whole rock MgO vs FeO* (calculated as 90% of total whole rock Fe expressed as FeO) for entire database, showing filtering of low-P plagioclase-present fractionation trend defined as samples plotting above the diagonal heavy dashed line. Diagonal grey lines are melt compositions in equilibrium with olivine of indicated Fo content based on the Roeder and Emslie (1970) Fe/Mg K_D value of 0.3 for olivine-liquid equilibrium. B. Plot of whole rock TiO_2 vs MgO (weight percent, recalculated to 100% volatile free) showing the classification into "komatiite", "picrite", "high-Ti basalt" and "low-Ti basalt" chemical groupings independent of provenance.

IPGEs and Mg#, but at systematically lower levels than in komatiites. In contrast, Pt and Pd show overall unsystematic variation, although variation with rock-type is evident. There is a weak negative correlation in komatiites between Mg# and both Pt and Pd and as with IPGEs, CLIP and OIB picrites are systematically depleted for the same Mg#. Basalts of all provenances show a wide range in Pt and Pd with no relationship to Mg#. The behaviour of Rh, typically, is intermediate between the IPGE and Pt–Pd groups; the distribution of Rh in komatiites is almost identical to that of Pt, while it shows a well developed positive correlation with Mg# in the CLIP data similar to that shown by the IPGEs. MORBs are consistently depleted in all PGEs. Bushveld sill samples are at the upper end of the range for all PGEs for given Mg#, and are notably enriched in Rh and Pt.

Considering inter-element correlations among the PGEs, (Figs. 3 and 4), the strongest correlations over the entire dataset are observed between Pt and Pd ($r = 0.77$ over the 675 samples passing the FeO–MgO screen), Ir and Ru (0.76), Ir and Os (0.67), Pt and Rh (0.65) and Pd and Rh (0.52), whereas correlations between IPGE and Pt or Pd are weak to nonexistent. The IPGEs Ir, Os and Ru show strong positive correlations ($r > 0.5$) with Mg#. Restricting the datasets to specific rock-types and settings enhances some of these correlations and diminishes others (Table 1). For komatiites only, Pt and Rh are more strongly correlated ($r = 0.76$ over 294 samples) as are Pd and Rh (0.63) while IPGE correlation coefficients decrease slightly. For continental LIPs only, combining high-Ti, low-Ti basalts and picrites, correlations among the IPGs remain strong ($r > 0.6$ over 489 samples), Pt and Pd remain very strongly correlated ($r = 0.8$), but the correlation between Pt and Rh diminishes ($r = 0.29$). A significant correlation appears in this grouping between Ir and Rh. Correlations between Mg# and Ir, Ru and Rh become more significant (0.66, 0.78, 0.54 respectively).

Further insight into the behaviour of the "incompatible PGEs" (in the sense of being incompatible in olivine) Pt, Pd and Rh is gained by plotting PGE/Ti ratios against Mg#, with the intent of removing the effects of extraction or addition of olivine during melting or crystallization processes (Fiorentini et al., 2010). This clarifies the trends considerably, particularly for komatiites. Ratios are normalized to estimated values for "primitive mantle" based on estimates for PGEs from Becker et al. (2006) and for Ti from McDonough and Sun (1995). The ratios Pt/Ti and Pd/Ti are approximately constant with Mg# for komatiites and most Archaean greenstone belt basalts; Rh/Ti behaves similarly but decreases slightly with decreasing Mg#. Komatiitic to picritic samples from Proterozoic terranes are systematically slightly depleted relative to Archaean komatiites. Continental LIP samples also show mostly horizontal trends consistent with incompatible (or weakly compatible in the case of Rh) behaviour, but are systematically depleted in Pt, Pd and Rh compared with komatiites. A scatter toward strongly Pt, Pd and Rh depleted samples is evident among high-Ti basalts from CLIPs; these are generally regarded as having undergone sulfide saturation and segregation in the crust, possibly related to ore formation in the case of basalts from Noril'sk (Brügmann et al., 1993; Lightfoot et al.,

Please cite this article as: Barnes, S.J., et al., Platinum group elements in mantle melts and mantle samples, Lithos (2015), http://dx.doi.org/10.1016/j.lithos.2015.07.007

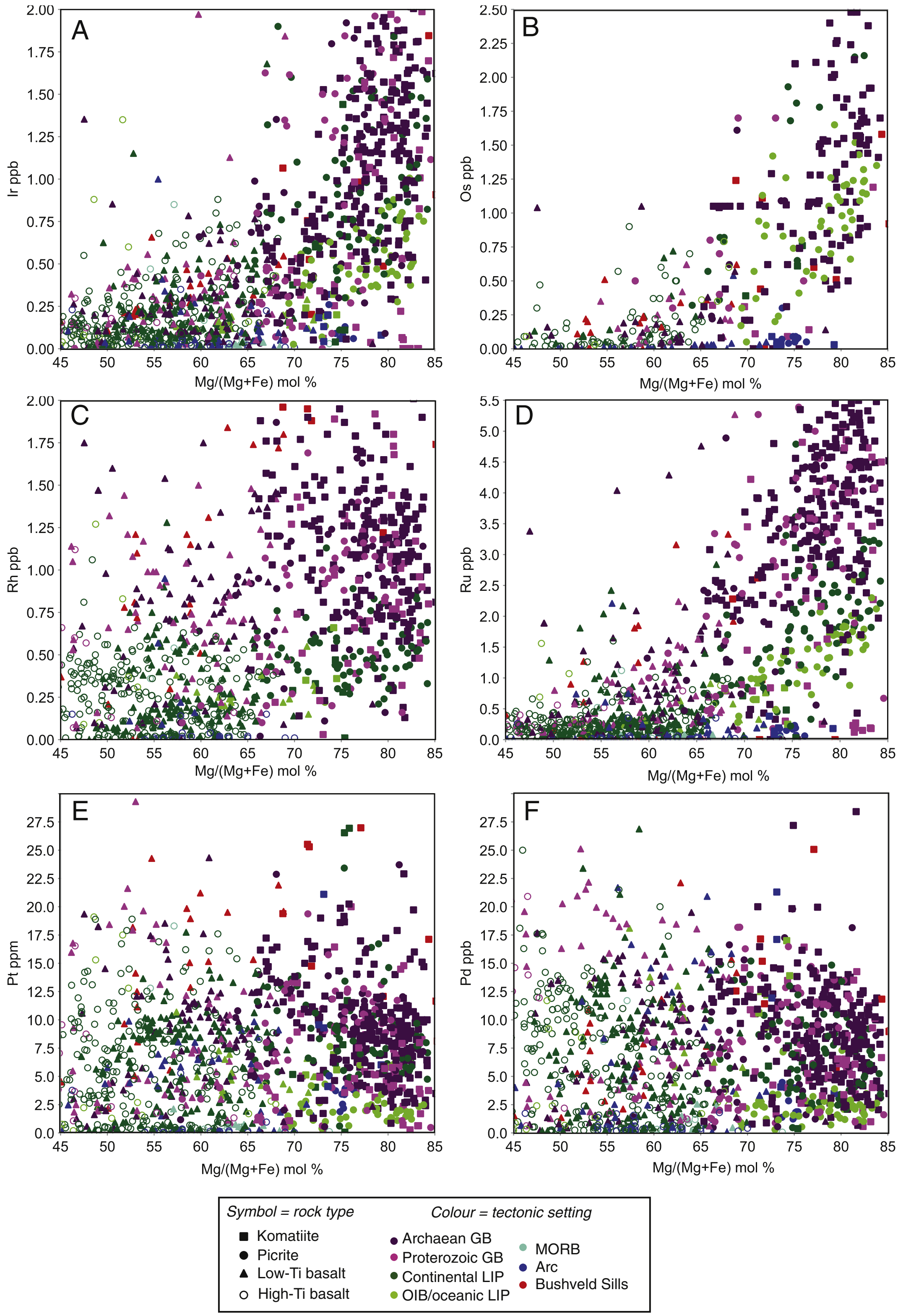

Fig. 2. Plots of PGE concentrations (ppb) vs Mg number (MgO / [MgO + FeO*]) for mantle melt samples passing the low-P FeO–MgO fractionation filter defined in Fig. 1. GB = greenstone belt, LIP = large igneous province, MORB = mid-ocean ridge basalt.

1992; Naldrett et al., 1992) and Raglan (Barnes and Picard, 1993). The same depletion is evident in MORBs, and in some samples from the OIB dataset. Strong depletion is also present in the OIB picrite set.

Variation in inter-PGE ratios in different rock types and settings is illustrated in plots of Pt/Rh, Pt/Ir and Pt/Pd in Fig. 5, and in multi-element spidergrams (Fig. 6), including Ni and Cu for context with other chalcophile elements, and Ti to indicate relationship to a representative olivine-incompatible element. The ratio Pt/Ir increases with decreasing Mg# from basalts to komatiites, with no particular relationship to setting or rock type. In contrast, while Pt/Rh also increases in the same

Please cite this article as: Barnes, S.J., et al., Platinum group elements in mantle melts and mantle samples, Lithos (2015), http://dx.doi.org/10.1016/j.lithos.2015.07.007

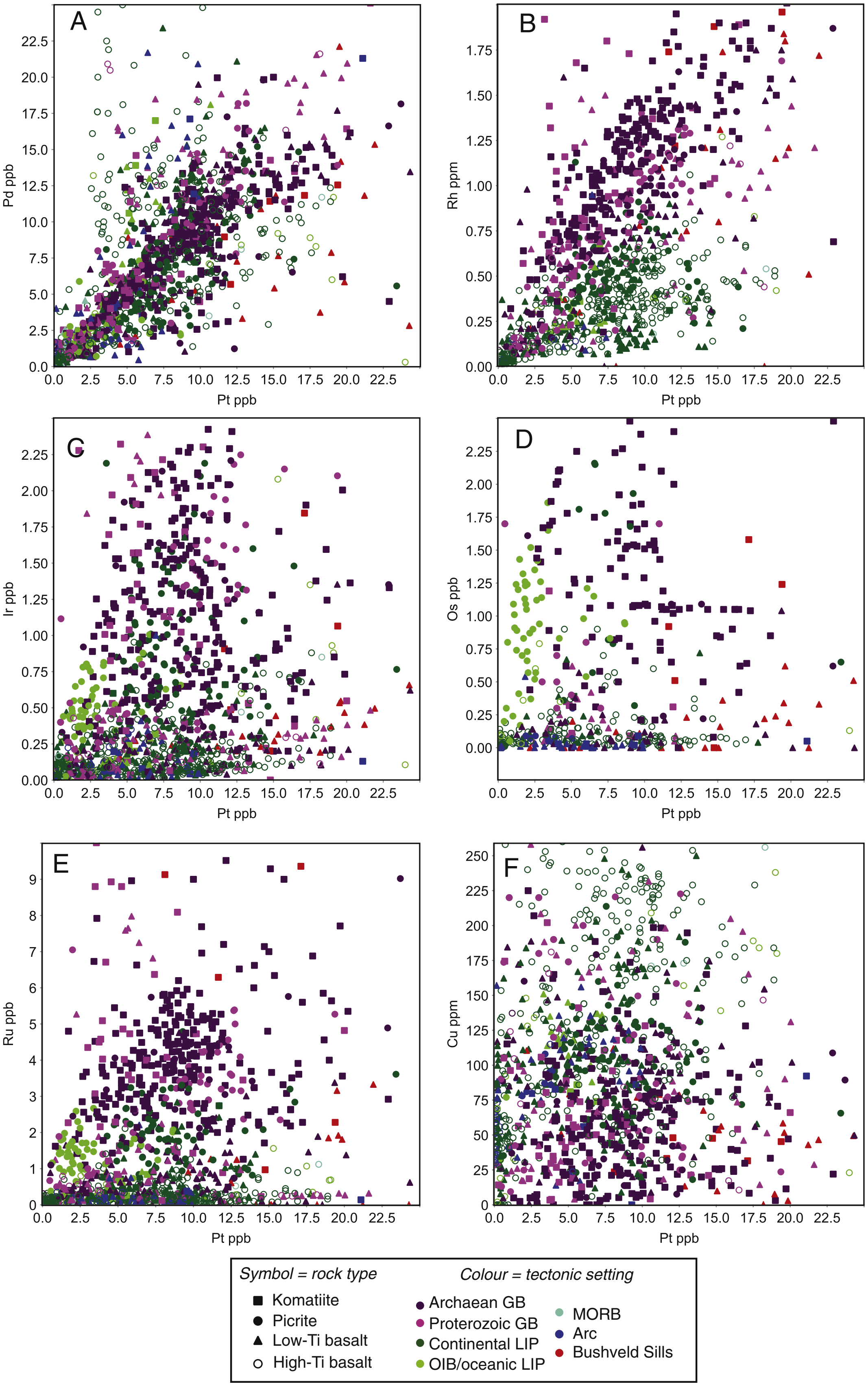

Fig. 3. Plots of PGE concentrations (ppb) vs Pt for mantle melt samples passing the low-P FeO–MgO fractionation filter defined in Fig. 1.

Please cite this article as: Barnes, S.J., et al., Platinum group elements in mantle melts and mantle samples, Lithos (2015), http://dx.doi.org/10.1016/j.lithos.2015.07.007

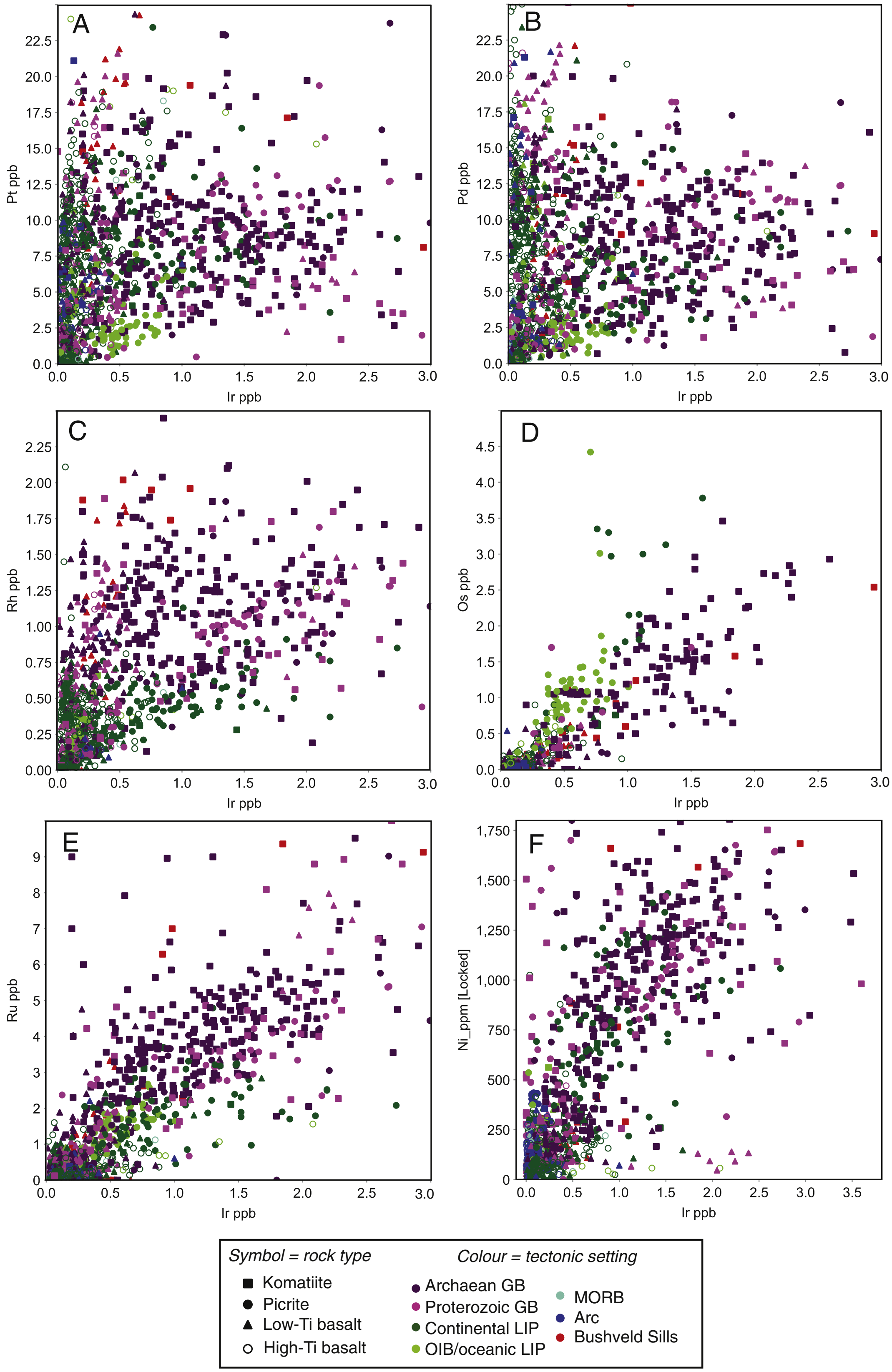

Fig. 4. Plots of PGE concentrations (ppb) vs Ir for mantle melt samples passing the low-P FeO–MgO fractionation filter defined in Fig. 1.

sense, there is a systematic offset between trends for komatiites and Archaean basalts, and for continental LIPs (regrettably there is insufficient Rh data for the other groupings). This further reflects the point made above from correlation coefficients that the relative coupling of Pt and Rh changes between these settings: Rh behaves more like an IPGE in basaltic and picritic magmas, and more like Pt and Pd in

Table 1
Correlation matrices, mantle melts. Correlation coefficients greater than 0.5 shown in bold.

Correlation	Ir	Os	Ru	Rh	Pt	Pd	TiO_2	Mg#
Mantle melts — all groupings								
Ir	1	**0.67**	**0.76**	0.4	0.22	0.16	−0.29	**0.57**
Os		1	0.37	−0.15	−0.019	−0.065	−0.05	**0.53**
Ru			1	**0.65**	0.35	0.28	−0.48	**0.55**
Rh				1	**0.65**	**0.52**	−0.45	0.27
Pt					1	**0.77**	−0.28	−0.053
Pd						1	−0.29	−0.085
TiO_2							1	−0.32
Mantle melts — komatiites only								
Ir	1	**0.66**	**0.6**	0.25	0.093	0.068	0.091	0.3
Os		1	0.12	−0.09	−0.2	−0.23	−0.26	0.35
Ru			1	**0.56**	0.31	0.24	−0.086	0.22
Rh				1	**0.76**	**0.63**	0.095	−0.12
Pt					1	**0.7**	0.29	−0.24
Pd						1	0.22	−0.2
TiO_2							1	**−0.52**
Mantle melts — CLIPs, all basalts and picrites								
Ir	1	**0.84**	**0.71**	**0.63**	0.24	0.11	−0.01	**0.66**
Os		1	0.13	−0.042	−0.026	0.71	−0.35	0.33
Ru			1	0.48	0.25	0.035	−0.11	**0.78**
Rh				1	0.29	0.26	0.014	**0.54**
Pt					1	**0.8**	0.086	0.066
Pd						1	−0.09	−0.047
TiO_2							1	−0.24

komatiites and associated Archaean basalts. The behaviour of Pt and Pd is strongly coherent across the entire dataset, notwithstanding some scatter, mainly in komatiites, possibly due to selective mobilization of Pd during alteration (Barnes and Liu, 2012). The only groupings showing consistent enrichment of Pd over Pt are high- and low-Ti MORBs (Fig. 6C and D).

A distinctive feature on the plots of PGE/Ti ratios vs Mg# is the distinctively PGE-enriched character of the Bushveld Sill compositions. Relative to the undepleted komatiite–basalt trend, the Bushveld B1 magmas are enriched over Ti by factors of about 2 for Pt and Rh and 1.5 for Pd. This enrichment does not appear to extend to Ir, Ru and Os, as is evident from Fig. 4 and from the spidergram plots in Fig. 6. Fig. 6A shows that the Bushveld patterns are generally similar to those for komatiites except for being relatively enriched in Pt and Rh and slightly depleted in Ni, Os and Ir (although not Ru). This is the only data set plotted here that is characteristically enriched in Pt over Pd. The same characteristic is seen in the Pt–Pd enriched siliceous high-Mg mafic magmas of the Vestfold Hills locality (Seitz and Keays, 1997) in Antarctica (these were not included in this compilation owing to a lack of complete major element data).

Some other generalities about different rock types and tectonic settings can be made from Fig. 6. Picrites from Proterozoic settings have similar PGE patterns to komatiites but generally high Cu, associated with higher Ti by definition. Ocean island picrites (primarily from Hawaii) have lower levels of PGEs overall, flat IPGE patterns with somewhat anomalous high Os/Ir, distinctly depleted Pt and Pd, and anomalously high IPGE/(Pt + Pd). Both low-Ti and high-Ti basalts from ocean islands have steep PGE patterns upward from Ir to Pd, and mildly depleted PGEs relative to Ni, Cu and Ti relative to average mantle. PGE patterns in MORBs are broadly parallel to those in high-Ti OIBs, but substantially more depleted. MORBs and high-Ti basalts from CLIPs and Archaean greenstone belts differ from other groupings in having relative depletion of Ru over Ir (i.e. downward slopes from Ir to Ru). High-Ti and low-Ti basalts from OIBs have otherwise similar IPGE patterns and levels, but high-Ti basalts appear to be more depleted in Pt and Pd; however, this may be an artefact of a small sample size. In CLIPs, low-Ti basalts are generally depleted in IPGEs relative to high-Ti basalts, but the opposite appears to be true for Pt and Pd. In both the plume-related data sets (CLIPs, OIBs) high-Ti basalts are more depleted in Pt and Pd than low-Ti basalts. Archaean basalts have generally similar PGE patterns to CLIP basalts, except for having higher Ru and Rh contents.

3. PGEs in mantle samples

The data set considered here was selected according to broadly similar principles as that for the mantle melt dataset, comprising high quality analyses collected in the last 15 years or so. The range of elements reported in mantle studies varies widely; a large number of recent studies report Os only in the context of Re–Os isotopic investigations and regrettably few of these studies report the other PGEs as well. Such data are included on plots where possible. As with mantle melts, Rh and Os are missing in many (different) samples according to the analytical protocol. Chromite-rich samples have been avoided to eliminate the well known affinity of IPGE-rich phases with chromitites.

The data set presented here overlaps with that reported by Lorand et al. (2012) and Aulbach et al. (2015), and this contribution is not intended to repeat the very comprehensive review of PGE and Re contents of subcontinental mantle samples in those papers, to which the reader is referred for detailed considerations of processes of mantle metasomatism and mineralogical deportment of PGEs in the mantle. The following discussion emphasises the more general trends evident in the entire data set, and compares the subcontinental (cratonic) data set with data from other well-represented settings. In the following section we use the relative strength of interlement correlations between the different PGEs to make deductions about the mantle melting processes that give rise to the signals discussed above in the mantle melt dataset.

In Fig. 7 we show PGE abundances versus Al_2O_3, which is an approximate proxy for degree of melting. Although the rate of Al_2O_3 depletion varies as melting reactions change with increasing pressure (Walter, 1998), it is convenient to regard Al_2O_3 concentrations between 2.5 and 4.5 wt.% as being relatively fertile, whereas samples with less than 2.5% Al_2O_3 have undergone large degrees of partial melting. Figs. 8, 9 and 10 show inter-PGE variations along with correlations for selected subsets of the data.

Over the mantle data set as a whole, the strongest correlations are between Ir, Ru and Os on one hand, and between Pt, Pd, and Rh on the other (Table 2). Distinct variations on this theme are seen within the major sub-divisions (Figs. 7, 8, 9,and 10).

3.1. Orogenic samples

This grouping consists of obducted "Alpine" peridotite complexes in orogenic belts and contains mostly lherzolites and a lesser number of harzburgites. Whereas the mantle section of ophiolites typically represents the shallow apical portion of the MORB melting prism and many ophiolitic peridotites have undergone severe melt depletion (e.g., Becker et al., 2006; Rehkämper et al., 1999), the obducted orogenic mantle massifs are widely thought to represent asthenospheric mantle that was incorporated into the subcontinental lithosphere at considerable depth by conductive cooling, hence avoiding adiabatic melt extraction during its addition to the lithosphere (e.g., Fabriès et al., 1998). Therefore this group of samples may offer the best opportunity to examine the composition of the convecting upper mantle. However textures displayed by some of these samples have been taken as evidence for mantle metasomatism and refertilization as a result of percolation of low-degree mantle partial melts, as also documented in a number of meticulously detailed studies of PGE and PGM residence at microscopic scale (Alard et al., 2000; Lorand et al., 2008c, 2010; Luguet et al., 2007a, 2007b). Whether or not this group of rocks preserves pristine upper mantle compositions, they form a convenient reference group that shows considerable overlap with the more fertile members of all the other peridotite groups. In an effort to see through the veil of partial melting and mantle metasomatism, we have filtered the orogenic peridotite data set to produce a subset of preferred compositions for the convecting

Please cite this article as: Barnes, S.J., et al., Platinum group elements in mantle melts and mantle samples, Lithos (2015), http://dx.doi.org/10.1016/j.lithos.2015.07.007

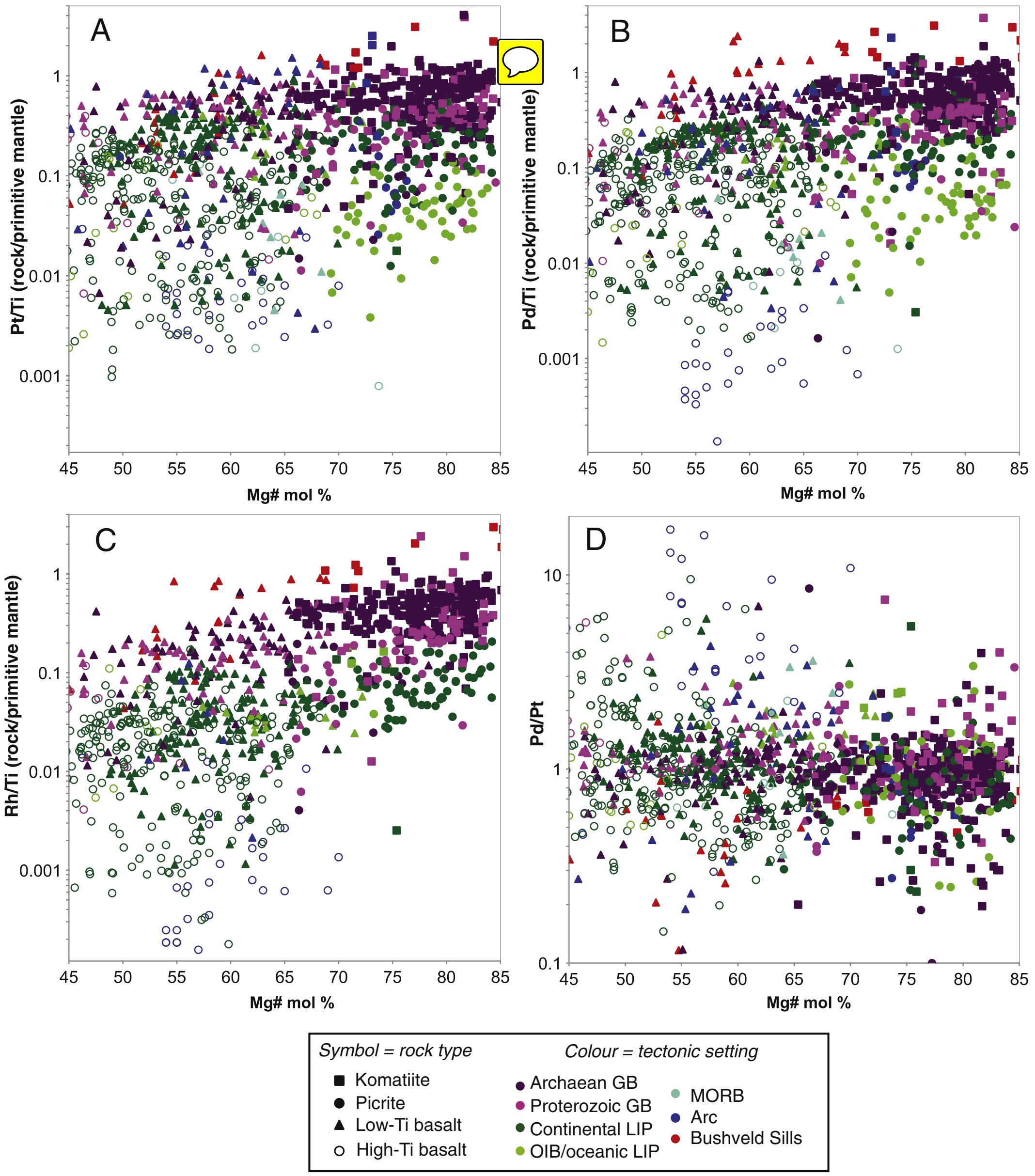

Fig. 5. Plots of PGE inter-element ratios vs Mg number (MgO / [MgO + FeO*]) for mantle melt samples passing the low-P FeO–MgO fractionation filter defined in Fig. 1.

upper mantle. To do so we first separated them on the basis of Al_2O_3 contents, retaining those with $2.5 < Al_2O_3 < 4.5$ wt.% (anhydrous) and labelling the rest as either "Al_2O_3-enriched" or "-depleted". Then to focus our attention on those samples that had not suffered obvious perturbation of their Pt and Pd contents away from the main population, we screened out any sample containing >8 ppb Pt or >7 ppb Pd, labelling those as "PGE-enriched". The remaining samples, representing our preferred representatives of the convecting mantle, are referred to in Figs. 7 to 10 merely as "orogenic". Also shown in each panel of Figs. 8,9 and 10 is an ellipse representing the 95% confidence interval calculated based on classic analysis of variance (i.e., ANOVA) for the filtered orogenic population. In the same Figures we have plotted the medians for the filtered orogenic suite as well as robust non-parametric regression lines drawn through these median values with slopes determined by Thiel–Sen analysis (Sen, 1968). All of the robust regressions pass very close to the origin. The median values are presented in Table 3.

The Al_2O_3-depleted orogenic suite shows a very broad scatter in all PGE abundances in Fig. 7. On average they appear to preserve IPGE concentrations similar to those of the filtered group of fertile orogenic samples, whereas there is perhaps some more scatter to mild depletions in Pt and Pd with decreasing Al_2O_3. The orogenic peridotites classified as "enriched" in either Pt or Pd show greatly enlarged scatter in the other PGE, giving some justification for their exclusion from the preferred data set.

3.2. Cratonic (subcontinental lithospheric) mantle samples

The cratonic mantle sample set consists dominantly of peridotitic xenoliths from kimberlites and alkali basalts and is taken to be the best available sample of the sub-continental lithospheric mantle under the Archean cratonic blocks. This sample set is the prime source of samples from which Re–Os model ages of subcontinental mantle lithosphere have been obtained (e.g., Griffin et al., 2004). Compositions range from a few "fertile" or undepleted peridotites and pyroxenite through to extensively melt-depleted harzburgites and dunites which constitute the vast majority of the cratonic suite. The cratonic suite distinct from all others in having strongly depleted Pt and very strongly depleted Pd relative to IPGEs, along with moderate depletion in Rh and little or no depletion in Au. These depletions are most evident in the

Please cite this article as: Barnes, S.J., et al., Platinum group elements in mantle melts and mantle samples, Lithos (2015), http://dx.doi.org/10.1016/j.lithos.2015.07.007

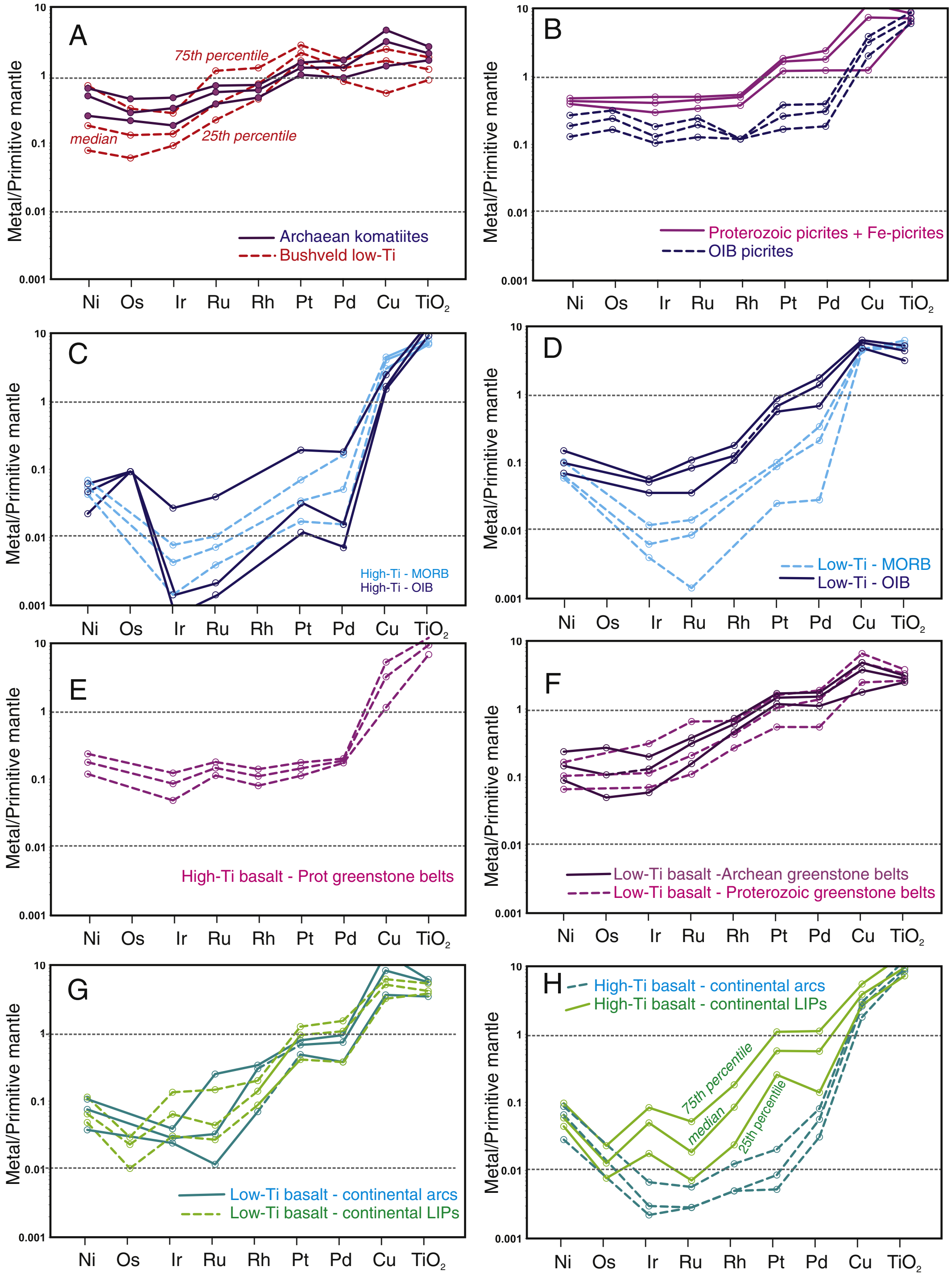

Fig. 6. Multi-element spidergrams in mantle melt sample categories for PGEs, Ni, Cu and TiO_2 relative to Becker et al. (2006) (PGEs) and McDonough and Sun (1995) (other elements) primitive upper mantle estimates. Median, 25th percentile and 75th percentile on each element in each group.
© 2015 CSIRO. All Rights Reserved.

most depleted samples, i.e. these samples with low Al_2O_3 (Fig. 7). The IPGEs, particularly Ir and Os (Fig. 9) are strongly correlated with one another, implying that they have behaved as a coherent suite during melt extraction, and the IPGEs are almost completely decoupled from Pt, Pd and Rh. The correlation between Ir and Ru is less strong in the cratonic data set than in the other groupings. PGE data show a large amount of scatter, perhaps owing to the small sizes of these predominantly xenolithic samples. However some broad generalizations are possible. Compared with the filtered orogenic group, the cratonic suite is extremely depleted in Pd but only moderately depleted in Pt and Rh. Os and Ru are weakly depleted, but Ir is notably enriched. The only other group of samples that show a combination of Ir enrichment with Pt depletion is the Al_2O_3-depleted orogenic group.

3.3. Off-craton samples

This category is essentially the same as that employed by Lorand et al. (2012), with the exception that samples of obducted “Alpine” peridotite massif complexes in orogenic belts are broken out as a separate category designated “orogenic”. Off-craton samples for the most part

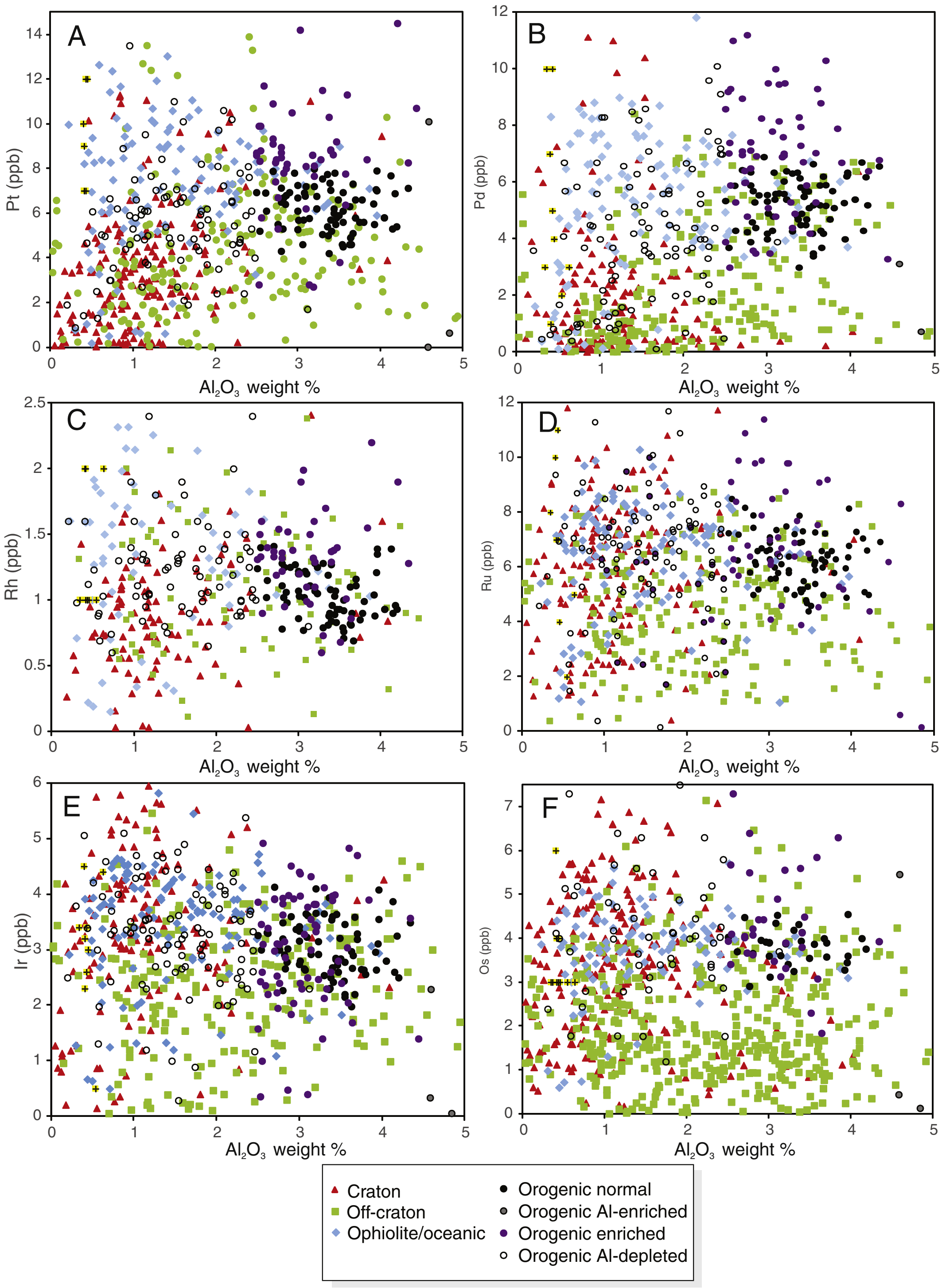

Fig. 7. PGE concentrations (ppb) vs Al_2O_3 content (weight percent), in mantle sample dataset.
© 2015 CSIRO. All Rights Reserved.

are ultramafic xenoliths, hosted by alkalic or peralkaline volcanic rocks, derived from crustal domains on the margins of or away from the ancient Archaean cratons: "Archons" of Begg et al. (2010).

Although both the cratonic and off-craton xenolith suites have been sampled from subcontinental lithosphere, they show some marked differences in PGE distribution. Like the cratonic suite, the off-craton suite shows depletions in Pt and all of the IPGE at all Al_2O_3 concentrations, and shares with the cratonic suite a dramatic Pd depletion, especially for the most melt-depleted samples. The key difference with the cratonic suite is that Ir is strongly depleted in the off-craton suite but not in the cratonic suite. This tendency for Ir to 'break ranks' with the other IPGE is evident in the pronounced cloud of red symbols at the lower right of Fig. 8C,D, and E; to a lesser extent this sector of the diagram is also populated by the melt-depleted Al_2O3-poor orogenic suite, suggesting an affinity between the cratonic and melt-depleted orogenic groups.

Abundance patterns overall are relatively flat and near-chondritic, particularly in the less Al-depleted samples (Fig. 11). Comparison of chondrite normalized PGE patterns between the top and bottom Al-quartiles (Fig. 11D) shows similar abundances of IPGEs, mild depletion of Pt and strong depletion of Pd in the Al-depleted samples. There is

Please cite this article as: Barnes, S.J., et al., Platinum group elements in mantle melts and mantle samples, Lithos (2015), http://dx.doi.org/10.1016/j.lithos.2015.07.007

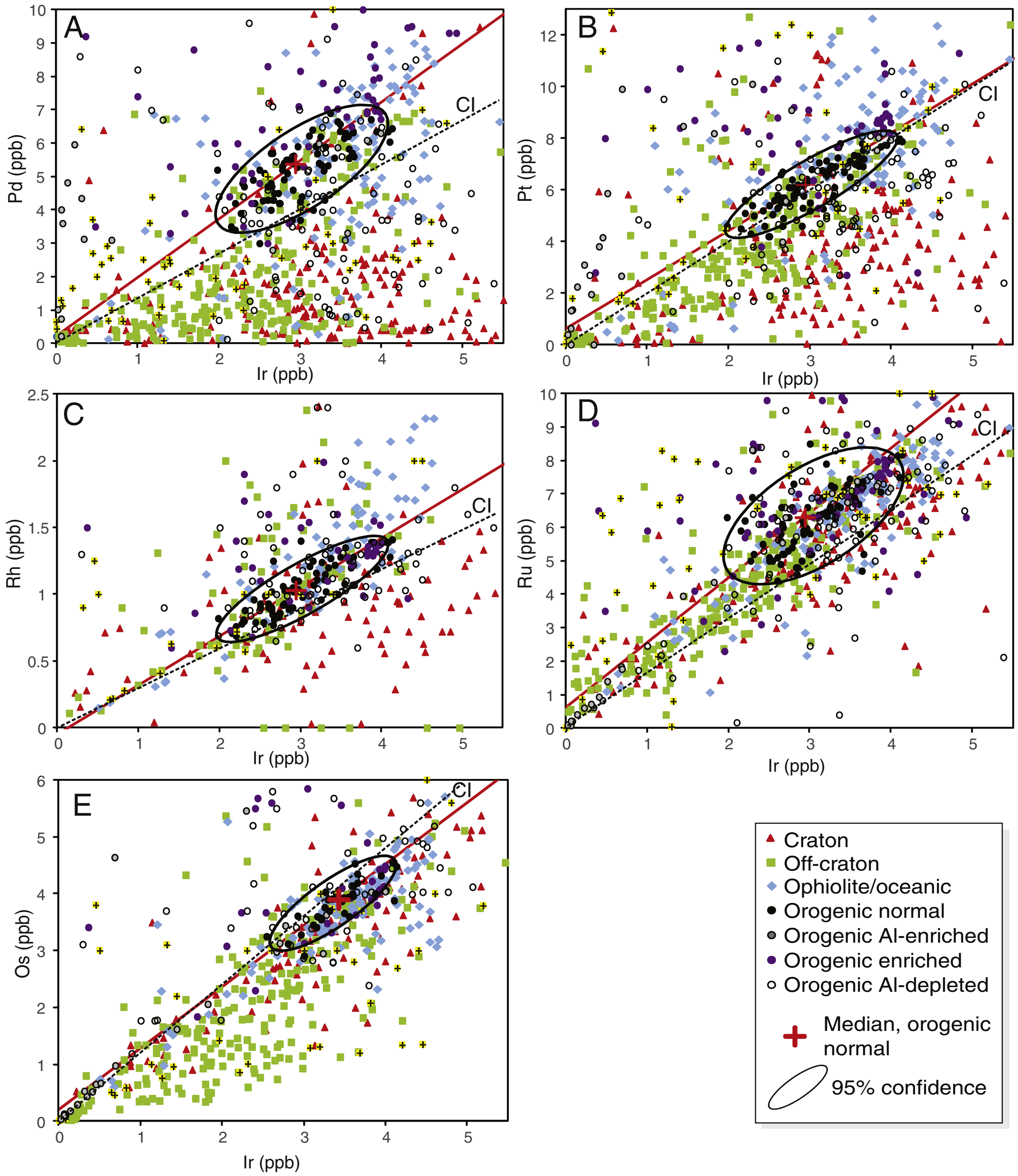

Fig. 8. Plots of PGE concentrations (ppb) vs Ir for mantle samples. Diagonal dashed lines show ratios for Becker et al. (2006) primitive mantle (PM) and CI chondrites (McDonough and Sun, 1995). Red crosses show median values for the filtered orogenic peridotite data; solid red diagonal lines pass through these medians with slopes determined by robust non-parametric regression using a bootstrap method, and black ellipses show 95% confidence intervals on the filtered orogenic samples using classic analysis of variance assuming normally distributed errors. We emphasize that the regression lines pass nearly through the origins of all plots, consistent with the presence of highly correlated errors in the data.

no depletion in Rh in the most Al-depleted samples relative to the least. Depletion in Pd extends to higher Al contents than in cratonic mantle samples (Fig. 7A). Ratios of Ir to Os are more variable, and generally higher, than in other categories. The Al-depleted off-craton sample pattern is similar to that for the entire cratonic dataset.

There is a moderate but significant correlation between Pt and both Ir and Ru in this group, particularly if the most Al-depleted samples are excluded (Fig. 10). The correlation coefficient for Pt and Ir within the upper two quartiles of Al content in this group is over 0.5 (table).

3.4. Oceanic and ophiolitic samples

Most of the samples in this subset are samples of ophiolitic harzburgite or lherzolite mantle, along with some xenoliths from oceanic settings. Compared with the filtered orogenic peridotite grouping, the oceanic and ophiolite samples have depleted Al_2O_3 but similar or slightly higher PGE concentrations, thus forming a cluster immediately to the left of the orogenic samples in Fig. 7. Clearly evident on the Pt and particularly Pd plots is a tendency to scatter toward elevated PPGE.

3.5. Arc mantle samples

The data set for arc mantle is sparse and suffers from extreme dispersion due most likely to very small sample sizes, but the available data do offer some interesting points of comparison with the other groupings. The very few samples for which Al_2O_3 concentrations have been reported are strongly melt-depleted harzburgites showing broad scatter in PGE but suggesting moderate enrichments in IPGE. Figs. 8,9 and 10 show that despite the scatter the arc samples tend to follow a pattern of depletion of all PGE relative to the filtered orogenic group, including Ir, resembling that shown by the off-craton suite but possibly distinct from the cratonic peridotites with their higher Ir concentrations.

Please cite this article as: Barnes, S.J., et al., Platinum group elements in mantle melts and mantle samples, Lithos (2015), http://dx.doi.org/10.1016/j.lithos.2015.07.007

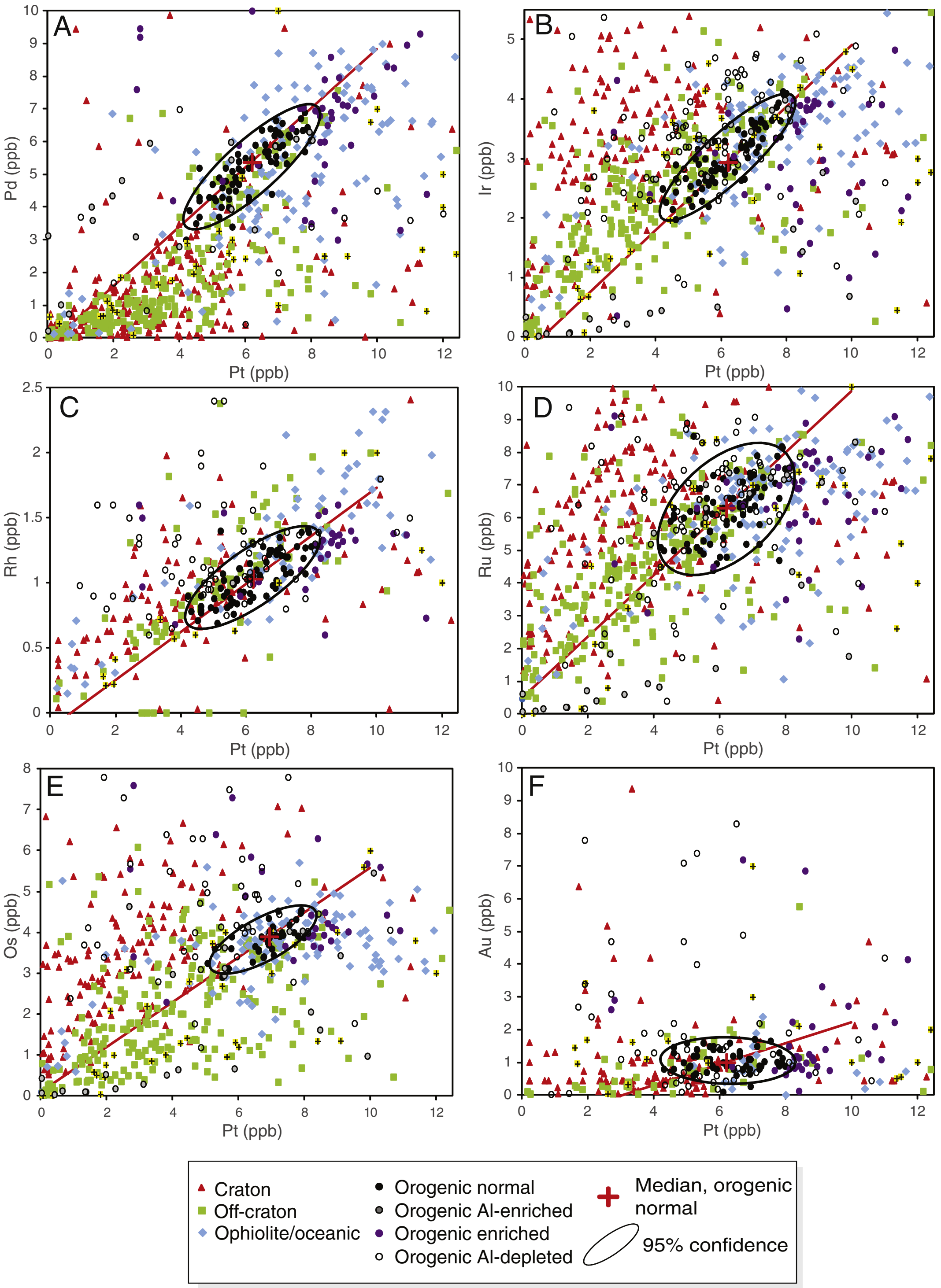

Fig. 9. Plots of PGE concentrations (ppb) vs Pt for mantle samples. Symbols as in Figure 8.

3.6. Cu/Pd and Cu/Pt ratios in the mantle

Variations in the ratios Cu/Pt and Cu/Pd are widely used in the literature on magmatic sulfide ore deposits, as indices of the degree and timing of sulfide liquid saturation in silicate magmas (Barnes et al., 2004a; Maier et al., 1996). Owing to the much higher partition coefficients from silicate to sulfide liquid both for Pt and Pd relative to Cu, segregation of even minute amounts of sulfide liquid from a silicate melt results in a rapid increase in both Cu/Pt and Cu/Pd, and this has been proposed as an exploration technique for magmatic sulfide mineralization and a fertility indicator for PGE mineralization in layered intrusions (Maier et al., 1996). Normalization to mantle abundances provides a point of reference for identifying magmas that have remained sulfide-undersaturated both during and after their derivation by mantle partial melting.

The orogenic mantle dataset provides the most reliable data source for normalization (Fig. 12). Data are shown for the orogenic, cratonic, off-craton and ophiolitic data sets only, eliminating a small number of oceanic island and island arc samples. Sample numbers are limited owing to lack of Cu analyses for many samples. For the preferred orogenic mantle suite, median values for Cu/Pt and Cu/Pd are 4758 and

Please cite this article as: Barnes, S.J., et al., Platinum group elements in mantle melts and mantle samples, Lithos (2015), http://dx.doi.org/10.1016/j.lithos.2015.07.007

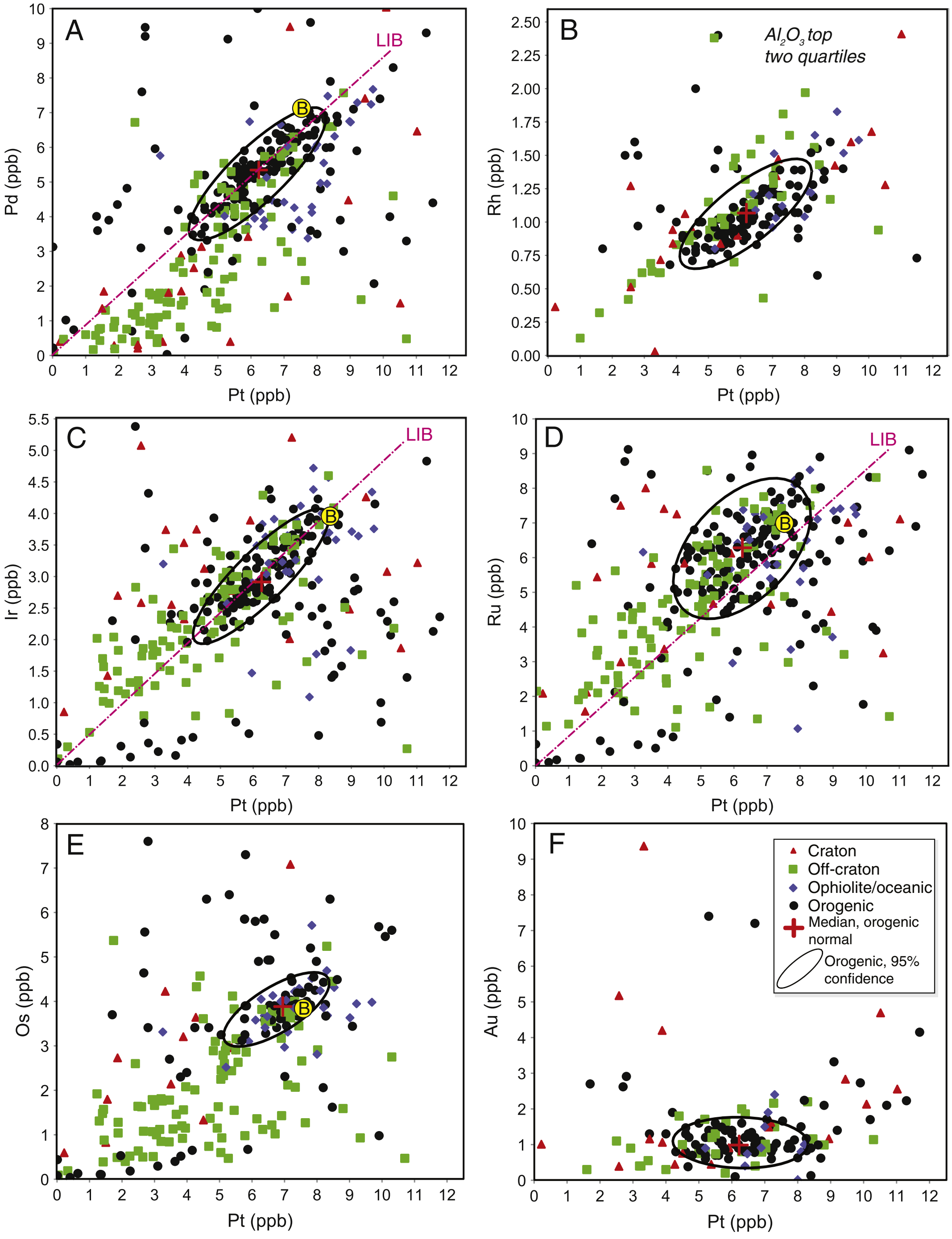

Fig. 10. PGEs vs Pt, mantle sample set restricted to Al-undepleted (Al in upper two quartiles) samples. Diagonal dashed line labeled 'LIB' represents lunar impact breccias (Norman et al., 2002). Yellow circle labeled 'B' is primitive upper mantle of Becker et al. (2006). Black ellipses and red crosses as in Figures 8 and 9.

5488 respectively, falling close to the peak contoured values for the overall mantle data set in Fig. 12.

4. Summary and interpretation of observations on natural data

4.1. Critical observations on mantle samples

4.1.1. PGE abundances in "average" mantle

The data for Pt and Pd in our filtered set of orogenic peridotites are shown in Fig. 13. Presuming that the least melt-depleted orogenic peridotites do indeed represent portions of the convecting mantle that have been incorporated passively into the lithosphere simply by conductive cooling through the base of the overlying continental crust, the medians of the PGE abundances of the filtered orogenic peridotite group might be taken as an estimate of the current composition of the convecting mantle (Table 3).

Acceptance of this value as representative of the convecting upper mantle requires that we account for the dispersal of measured compositions. We address three possible causes of the dispersal; metasomatism, partial melting, and sampling error. By filtering out samples with high Pt and Pd we have eliminated all obvious outliers; the medians we report would hardly be affected by including these outliers because of the strong clustering shown by the data closest to the median values. It appears unlikely to us that any metasomatic process could operate uniformly on

Table 2
Correlation matrices, mantle samples. Correlation coefficients greater than 0.5 shown in bold.
© 2015 CSIRO. All Rights Reserved.

All samples except 28 fliers on Pt–Ir

Correlation	Pt_ppb	Pd_ppb	Rh_ppb	Rua_ppb	Ir_ppb	Os_ppb
Pt_ppb	1	**0.66**	**0.54**	0.35	0.34	0.44
Pd_ppb		1	0.46	0.21	0.055	0.26
Rh_ppb			1	0.46	0.39	0.48
Ru_ppb				1	**0.72**	**0.6**
Ir_ppb					1	**0.73**
Os_ppb						1

Mantle samples, Al2O3 > 1.95 (top two quartiles), ~1% fliers on Pt/Ir removed

Correlation	Pt_ppb	Pd_ppb	Rh_ppb	Ru_ppb	Ir_ppb	Os_ppb
Pt_ppb	1	**0.65**	**0.54**	0.39	0.33	0.47
Pd_ppb		1	**0.58**	0.26	0.019	0.27
Rh_ppb			1	0.39	0.38	**0.58**
Ru_ppb				1	**0.81**	**0.65**
Ir_ppb					1	**0.78**
Os_ppb						1

Pt–Ir goes to 0.51 excluding fliers and taking out orogenic dataset.
Take out cratonic as well goes to 0.65 over ~300 samples

such a large scale that the entire central group of orogenic peridotites would move in concert to a new, altered composition; we prefer to attribute scatter to metasomatism away from a pristine original composition defined by the population medians. The degree of partial melting experienced by the most Al_2O_3-rich peridotites in the western Pyrenees was negligible, and their Al_2O_3 and lithophile trace element abundances (Fabriès et al., 1998) are very similar to the depleted MORB-source mantle of Salters and Stracke (2004).The effects of partial melting on fertile mantle lherzolite were addressed in detail by Mungall and Brenan (2014). The effects of removal of 5 wt.% basaltic melt along an adiabat are shown in Fig. 13 as a short heavy grey line. The change in mantle composition attributable to the amount of melt extraction these rocks have undergone is less than one tenth of the total range of values shown, indicating that the principal cause of the observed variation cannot have been melting.

We therefore need to address sampling error. A typical approach to sampling of orogenic peridotites for PGE is to obtain 1 kg samples from the field and crush them to coarse (~1 cm) chips, then take 100 g of chips and pulverize them to powders with grain sizes on the order of 10 to 75 μm (J.-P. Lorand, pers. comm. 2015). The spatial distribution of the PGE was probably established in the rocks while they resided in the asthenosphere at their solidus temperatures, in the presence of trace amounts of silicate melt and sulfide melt. At the grain sizes of typical granular to weakly protoclastic peridotites, former immiscible sulfide melts exist as small pockets ranging in size from tens of μm up to 500 μm in size (e.g., Luguet et al., 2003Fig. 1; Lorand et al., 2008b). Consideration of the cubic relationship between radius and volume shows that in a rock containing a variety of particle sizes, the vast majority of the mass of sulfide in the rock will reside in the few largest grains. For example, one grain 500 μm in diameter contains as much sulfide and contained PGE as 1000 grains 50 μm in diameter; it is therefore the distribution of only the very largest observed sulfide grains (and indeed probably a few even larger unobserved grains) in a rock that is of interest. At the conditions of partial melting, Pt and Pd are quantitatively sequestered in sulfide melt, having negligible concentrations in all other phases. Coarse crushing of a rock containing sub-mm grains of sulfide does not comminute the sulfide grains, which instead remain locked inside the cm-sized chips. Therefore, taking a subset of these chips weighing 100 g is statistically indistinguishable from simply taking a 100 g sample of the whole rock.

According to simple mass balance considerations, a parcel of mantle peridotite containing 6.3 ppb Pt and 100 ppm S would have a volumetric modal abundance of 0.03% sulfide liquid containing 22 ppm Pt. Using spreadsheet software to estimate sampling error (Stanley, 2003) we find that the relative error of Pt concentration for this situation is 13 relative % if the sulfide resides in 350 μm bodies in a 100 g sample; if the sulfide grain size is 500 μm the relative sampling error rises to 22%, but if the sulfide is more uniformly dispersed in 100 μm grains the error falls to only 2%. We have used these estimates of relative error combined with the reported reproducibilities of PGE analyses on repeat analyses of individual sample powders (Fischer-Gödde et al., 2011) in a Monte Carlo simulation of sampling error for 100 g samples of orogenic peridotite. The simulations were carried out on 10,000 normally distributed random samples for sulfide particle radii of 10, 100, 250, 350, and 500 μm. The 95% confidence ellipses on each of the simulated data sets are shown along with a subset of 200 such random samples for the 350 μm case in Fig. 13. The extreme covariance of Pt with Pd in the 500 and 350 μm models matches well with the observed natural covariance, whereas in the case of 10 and 100 μm sulfide grain models the expected distributions show essentially no covariance. We conclude that the covariance shown on all of the inter-PGE plots in Figs. 8 to 10 is best accounted for by sampling error resulting from analysis of under-sized samples, whereas dispersal of data to either side of the regression lines results from analytical error as expressed by the reproducibilities. Pulverization of at least 1 kg of material would be required to attain sample errors controlled only by the reproducibility of the analytical techniques themselves and represented by the smallest ellipse in Fig. 13 unless the samples are much finer grained and more homogeneous than we have assumed. Although in many cases the orogenic peridotite samples presently have fine-grained protoclastic to mylonitic textures, there is ample textural evidence that this solid-state tectonic grain size reduction has merely spread the original sulfide bodies out into clouds of smaller particles which remain spatially associated within small volumes and hence would still fail to be comminuted by the early crushing stage of sample preparation. Hence the assumption of large sulfide grain size still holds for our purposes unless samples have been thoroughly mechanically mixed at the decimetre scale during tectonic transport.

Table 3
Estimates of PGE contents in undepleted mantle.
© 2015 CSIRO. All Rights Reserved.

	Preferred convecting mantle	Barnes et al.(1985) PUM	Becker et al.(2006) PUM	Puchtel et al.(2004) PUM	McDonough and Sun CI chondrites	Norman et al.(2002) lunar impact breccias
Os ppb	3.9	4.2	3.9	3.9	490	
Ir ppb	2.9	4.4	3.5	3.6	440	6.5
Ru ppb	6.3	5.6	7.0	5.4	710	11.7
Rh ppb	1.03	1.6			130	
Pt ppb	6.2	8.3	7.6	6.4	1010	13.7
Pd ppb	5.38	4.4	7.1	6.3	550	11.7
Cu/Pt	4758					
Cu/Pd	5488					
Pt/Ir	2.11	1.89	2.17	1.78	2.30	2.10
Pd/Ir	1.83	1.00	2.03	1.75	1.25	1.79
Pt/Pd	1.15	1.89	1.07	1.02	1.84	1.17
Ru/Ir	2.14	1.27	2.00	1.50	1.61	1.79

Please cite this article as: Barnes, S.J., et al., Platinum group elements in mantle melts and mantle samples, Lithos (2015), http://dx.doi.org/10.1016/j.lithos.2015.07.007

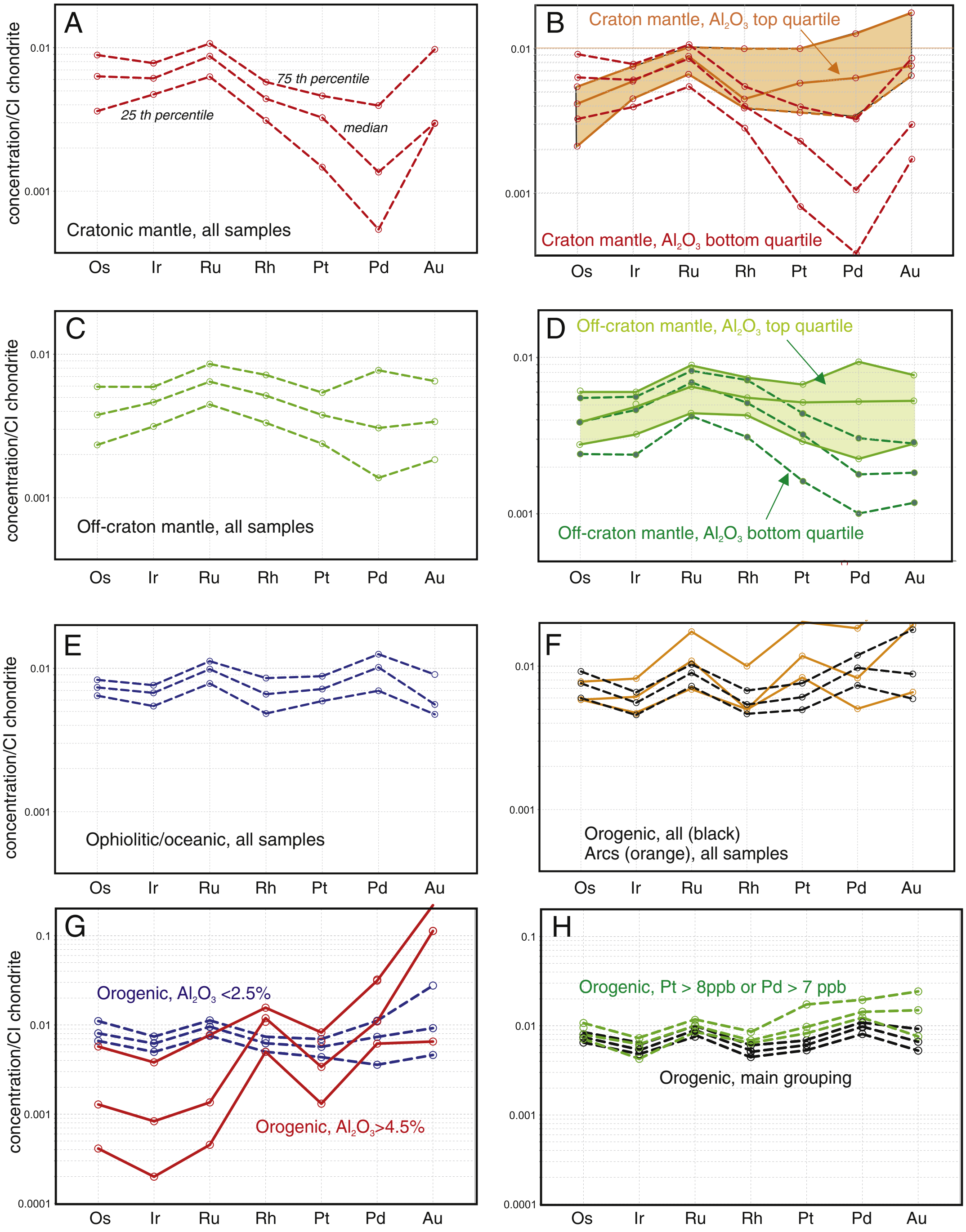

Fig. 11. A to E, multi-element spidergrams in mantle melt sample categories for PGEs, and Au relative to CI chondrite estimate from McDonough and Sun (1995). Median, 25th percentile and 75th percentile on each element in each group. G,H: data restricted to individual samples with anomalously high Pd (above the indicated dashed line) in the orogenic category. © 2015 CSIRO. All Rights Reserved.

Our statistical treatment implies that every data point in Figs. 8,9 and 10 should be represented by a marker about the size and orientation of the large black ellipses surrounding the orogenic data in each plot, scaled to their distance from the origin. Evidently the interpretation of trends through small sample sets is fraught with uncertainty, and only the gross behaviour of large clusters or clouds of data in our diagrams can be considered representative of large-scale mantle processes like melting. Even metasomatic signatures are likely to suffer extreme dispersion if the secondary phases have nuggety spatial distribution; the problem is even worse for sparsely distributed platinum group minerals such as PtFe alloy, with concentrations of Pt ranging as high as 80%.

The ultimate origin of the PGE controlling component in these samples remains a mystery, but the strong inter-element correlations suggest strongly that it is a sulfide component with a highly consistent composition but highly variable modal abundances at the scale of the samples analysed. It ultimately may be derived from an ancestral cumulus sulfide component during formation of mantle lherzolites as magma chamber or magma ocean cumulates; it may represent the “stirred in” PGE-enriched component of the Late Veneer (Chou, 1978; Chu et al., 2001; Lorand et al., 2008b; Morgan et al., 2001; Norman et al., 2002) or it may reflect other previously unrecognized processes. Some of the samples incorporated in the dataset may be cumulates from the transporting magma or may have been modified by reaction between mantle and percolating melts.

In Table 3 we compare our preferred composition of convecting upper mantle to previous estimates of the primitive upper mantle

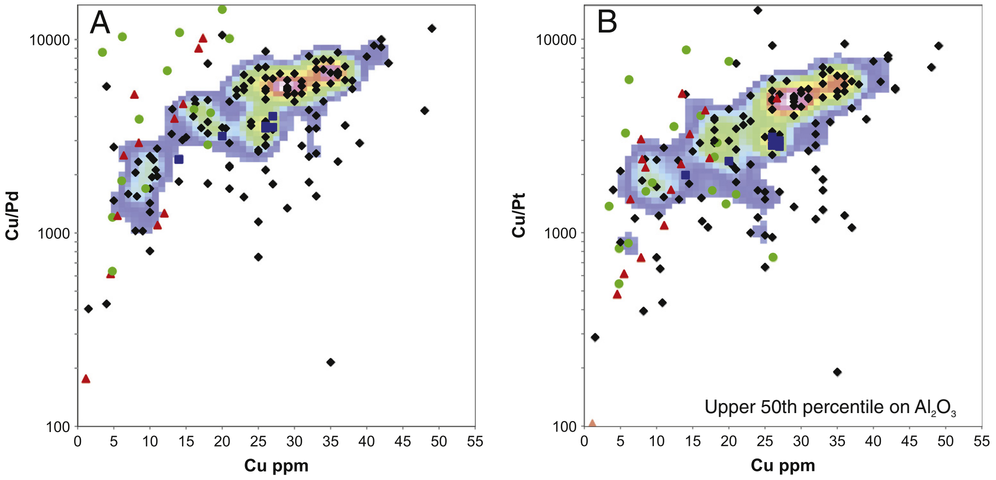

Fig. 12. Cu/Pt and Cu/Pd vs Cu for mantle samples with data density contours. Blue contour includes 80% of data.

(Barnes et al., 1985; Becker et al., 2006; Puchtel et al., 2004) and to CI chondrites (McDonough and Sun, 1995), which are commonly taken to resemble the bulk composition of the Earth, as well as lunar impact breccias (Norman et al., 2002), which may contain an endowment of PGE similar to what was added to the Earth as a late veneer after core formation.

There is a distinct departure in most of the PGE ratios in our preferred upper mantle composition compared to CI chondritic proportions, particularly for the case of Pt and Pd. As has been noted in previous studies (Becker et al., 2006; Fischer-Goedde et al., 2011; Pattou et al., 1996) the characteristic near-one-to-one ratio of the bulk of the undepleted mantle dataset is significantly different from the chondritic value of Pt/Pd around 2. Based on the very consistent 1:1 ratio of Pt:Pd in komatiites, the highest degree mantle melts available to sample, Puchtel et al. (2004) concluded that primitive mantle had 1:1 Pt:Pd and is hence non-chondritic with respect to Pt and Pd (Table 3). The mode of the mantle array also falls slightly on the low-Pt side of the chondrite line for Rh and Ru and (very slightly) for Os, but almost exactly coincident for Ir. These departures are attributed to a slight surplus of Pt and Ir and deficiency of Pd relative to the other PGEs. These surpluses and deficits were recognized by Becker et al. (2006) in making an estimate for bulk silicate earth PGE abundances, and the relative proportions in their estimate are shown as the “primitive mantle” line on the various scatter plots.

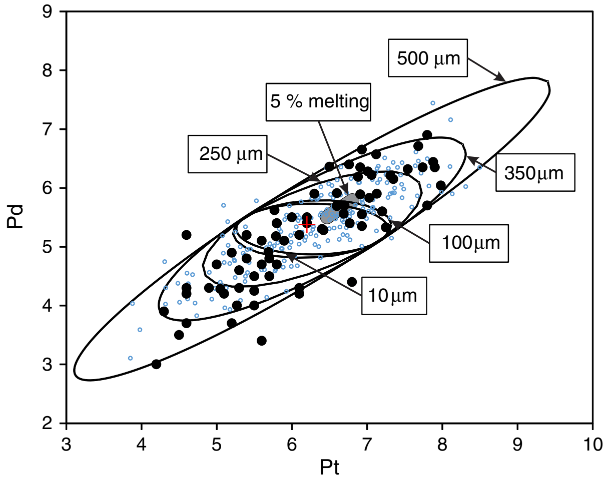

Fig. 13. Pd vs Pt for preferred orogenic peridotite samples. Black circles are data, blue dots are Monte Carlo simulation for 350 μm diameter sulfide grains. Solid black ellipse is the 95% confidence interval for actual data; thin black ellipses are 95% confidence intervals for Monte Carlo data sets for indicated sulfide grain sizes in 100 g sample containing 100 ppm S and 6.2 ppb Pt.

It has been recognized for at least a decade that relative abundances of PGE in the Earth's mantle resemble those of the late meteoritic bombardment as it is represented by lunar impact breccias (Norman et al., 2002). However previous estimates of primitive upper mantle inter-PGE ratios have matched neither CI chondrite values nor those of the lunar impact breccias. Ratios of Pt/Pd, Pt/Ir, and Pd/Ir for our preferred orogenic peridotite suite are effectively indistinguishable from those in lunar impact breccias (Table 3). The striking similarity between these two groups of samples considerably strengthens our proposal that our estimate captures the PGE abundances in the convecting upper mantle and supports the idea that the PGE were added to the mantle after core formation by the addition of meteoritic material (e.g., Maier et al., 2009). Ru/Ir in orogenic peridotites is less well matched to lunar breccias, however the Ru data are far more scattered than Pt, Pd, or Ir, and hence the significance of the discrepancy in Ru/Ir is hard to assess.

4.1.2. Are PGE mantle abundances dominated by refertilization processes?

The existence of Pd and Re enrichment signals in “refertilized” mantle samples, typically pyroxene-rich lherzolites or true pyroxenites, has been claimed by numerous detailed studies summarized by Lorand et al. (2012). However, the presence of a near-homogeneous sulfide component with PGE element ratios consistent with a late veneer component, in a significant proportion of samples in the mantle dataset, raises the question of how significant this process is in the PGE evolution of the crust-mantle system as a whole. If most lherzolite samples are the result of the refertilization of previously depleted harzburgite, then it requires a remarkable coincidence to add exactly enough Pt and Pd enriched metasomatic component to IPGE-rich, Pt–Pd- depleted harzburgite to bring the element proportions of such a high proportion of the sample set up to their characteristic and consistent proportions. The strong correlation of Rh with Pt in Al-undepleted mantle samples (Fig. 10B) is a key line of evidence here, in that Rh is expected to be concentrated in MSS rather than in the low-melting interstitial Pt–Pd component that has been identified with the metasomatic component. Rhodium and Pt should be effectively decoupled during metasomatic processes. Furthermore, depleted harzburgite is commonly strongly depleted in Pd over Pt, whereas these two elements are very strongly correlated in most mantle melts as we have seen. We conclude that while metasomatic signals are clearly evident in Al-enriched orogenic samples with elevated Pd (Fig. 11G), this is not a dominant contributor to the overall variability of the mantle dataset.

Please cite this article as: Barnes, S.J., et al., Platinum group elements in mantle melts and mantle samples, Lithos (2015), http://dx.doi.org/10.1016/j.lithos.2015.07.007

4.1.3. Where is the high Pd/Pt component complementary to Pd depleted subcontinental cratonic mantle samples?

We have seen that highly depleted, Al-poor samples of cratonic lithosphere are systematically strongly depleted in Pd over Pt. Mantle melts in contrast have very strongly correlative Pt and Pd, and have Pt/Pd ratios consistently close to 1:1 with the exception of some Bushveld magmas, and if we exclude Fe-enriched basaltic melts with high Pd/Pt due to low pressure fractionation. Whatever process has produced extensive depletion of Pd over Pt in the mantle is not the process that has generated the bulk of continental basalts. The only identifiable reservoir of Pd-enriched mantle material is the set of re-fertilized pyroxene-rich lithologies sampled within orogenic lherzolite complexes and ophiolites; these are probably formed by percolation of fluids generated at very low degrees of partial melting. The subset of Al-poor mantle samples with undepleted Pd consistently shows enrichment of Pd over Pt (Fig. 11G). The most aluminous upper 50% of the cratonic data set shows no systematic Pd/Pt enrichment (Fig. 11D), and the most likely samples of low-degree melts from subcontinental lithosphere, the MARID xenoliths, show no evidence for significant Pd enrichment either (Maier et al., 2015).

The only non-fractionated melt suite that shows consistently high Pd/Pt is MORB (Figs. 5F and 10); but this suite is also expected to have high Pt/Rh (Mungall and Brenan, 2014, Fig. 10 and references cited therein). Although the tectonic settings appear not to be compatible, it was suggested by Mungall and Brenan (2014) that the Kaapvaal subcratonic lithospheric mantle may have originated as the restite from low pressure melting with high potential temperatures to produce MORB-like picrites. This strongly melt-depleted residue may then have been accreted to the base of the lithosphere by lateral tectonics, possibly in a subduction environment. This material could account for the high Pt/Pd of the Kaapvaal mantle xenolith population (Maier et al., 2012a) and the high Pt/Pd of Bushveld magmas noted above. In this interpretation, the complement to the Pd depleted cratonic mantle material would be MORB. The missing Pd should be sequestered in whatever mantle reservoir presently contains foundered or subducted Archean crust that was extracted from the Kaapvaal subcontinental lithosphere. This suggestion does not distinguish between plate tectonic or other tectonic models for Archean ocean basins, but it does imply that the Kaapvaal lithosphere originated via low pressure melting in an ocean basin.

4.2. Pt and Pd behaviour in primitive basalts

Platinum and Pd behave as incompatible elements in komatiites in the absence of sulfide. However, there is a systematic decrease in Pt/Ti and Pd/Ti ratios from komatiites through to komatiitic basalts and low-Ti tholeiitic basalts in greenstone belt samples, which seems to indicate a mild compatibility of both elements (Fig. 5A, and B). Indeed, if Pt and Pd are genuinely incompatible elements in the absence of sulfide, then it is difficult to explain why apparently S-undersaturated basalts in general have lower Pt and Pd contents than komatiites; they should be higher, owing to lower degrees of partial melting and/or more advanced fractionation of non-Pt–Pd bearing silicates.

A plausible explanation was first suggested by Rehkämper et al. (1999) for MORBs and Momme et al. (2006) for plume-related basalts from east Greenland, and revisited by Mungall and Brenan (2014): basalts form by aggregation of melts extracted from the complete range of melting depths in a mantle domain undergoing adiabatic uplift and partial melting. Owing to the pressure dependence of S solubility (Mavrogenes and O'Neill, 1999), basalts arrive at the surface of the Earth in a state of sulfide undersaturation regardless of whether or not they were sulfide-saturated when they separated from their mantle source. However, during low-pressure adiabatic melting in ocean basins, sulfide liquid remains in the restite until the upwelling mantle has reached the shallowest part of the melting region. Therefore even apparently S- undersaturated basaltic magmas probably represent mixtures of highly PGE-depleted melt derived from the deeper parts of the melting column with small proportions of PGE-rich melt derived from the uppermost part of the melting column. In both the plume-related data sets (CLIPs, OIBs) high-Ti basalts are more depleted in Pt and Pd than low-Ti. This is interpreted as a result of lower degrees of partial melting forming high-Ti basalts, with a consequence that a higher proportion of sulfide is likely to be retained in the source, and a higher proportion of sulfide-saturated magma is incorporated into the integrated partial melt product over the range of melting depths. MORBs and high-Ti basalts from CLIPs and Archaean greenstone belts differ from other groupings in having relative depletion of Ru over Ir (i.e. downward slopes from Ir to Ru). A possible explanation is that magmas have fractionated chromite at some point in their evolution; Ru is much more compatible in chromite than the other IPGEs under typical mantle redox conditions (Brenan et al., 2012).

The data for CLIP and OIB show marked overall depletions in PGE relative to high degree melts of peridotitic mantle as represented by komatiites. The reasons for this probably lie in their derivation from different source material and possibly also from contamination en route to their sites of eruption in the case of the CLIP samples. It is widely acknowledged that the source mantle of OIB cannot have been ordinary peridotitic mantle; rather it has been supposed that a significant or even dominant portion of the source mantle for these suites comprises formerly subducted basaltic material which now exists as either eclogite or as pyroxenite derived from reactions between peridotite and eclogite-derived melts (e.g., Sobolev et al., 2005, 2007). There are insufficient experimental data to constrain properly the expected distribution of PGE during melting of eclogitic or pyroxenitic mantle. However we note that the basaltic crustal component, most likely MORB-like, which is thought to provide the raw material for deep mantle pyroxenite and eclogite, would be expected to be impoverished in PGE compared with the peridotitic mantle (Fig. 6). Melts of a mixture of peridotite and pyroxenite would thus be expected to be derived from a source that was PGE-depleted, simply due to dilution of the PGE-rich peridotite by PGE-poor eclogitic material.

4.3. IPGE and Rh behaviour in mantle melts

The IPGEs behave essentially as compatible elements in high degree partial melts such as komatiites, although the scatter is wide and unsystematic with respect to major element composition. Coupled with the wide variability observed in komatiitic olivine cumulates (not shown here), Barnes and Fiorentini (2008) concluded that the pattern of variability was the result of a decrease of IPGE solubility with falling temperature, for which Mg# is a proxy, coupled with sub-cotectic accumulation of IPGE-rich phases in cumulates. IPGEs are highly insoluble in silicate melts, and are less soluble in basalts than komatiites (Barnes and Fiorentini, 2008; Borisov and Palme, 1995; Brenan et al., 2005).

The IPGEs are strongly depleted in basalts regardless of the degree of depletion of Pt and Pd. Those samples that are depleted in Pt and Pd (based on Pt/Ti and Pd/Ti ratios compared with expected mantle values), and are therefore interpreted to have undergone extraction of a sulfide melt component, are also invariably depleted in the IPGEs as well, but low IPGE concentrations are also found in Pt and Pd undepleted samples. This is attributed to the solubility effect, and to the retention of IPGE-rich (IPGM) phases in mantle restite (Fonseca et al., 2012).

The experimental results on olivine-IPGE and Rh partitioning of Brenan et al. (2003, 2005) raise the possibility that olivine is a significant control on IPGE behaviour in addition to IPGM phases. However, if olivine control is dominant, it is difficult to explain the decoupling of Rh from the IPGEs in the melt composition data set, since Rh has similar partition coefficients into olivine as the IPGEs. This remains unexplained, but the answer may lie in the interplay between temperature, fO_2, alloy solubility and partition coefficients. This relationship is exerted through the tendency for magmas and their source mantle to

Please cite this article as: Barnes, S.J., et al., Platinum group elements in mantle melts and mantle samples, Lithos (2015), http://dx.doi.org/10.1016/j.lithos.2015.07.007

remain close to an internally buffered fO_2 parallel to one of the solid oxygen buffers like FMQ. Since fO_2 varies with temperature along such a buffer, and since both partition coefficients and alloy solubilities are controlled by fO_2 via redox reactions between metals and dissolved oxide cations of various valence states, temperature indirectly controls the partitioning of PGEs between melt, alloys and olivine. It is likely that IPGE concentrations in melts are subject to control by alloy solubility, olivine partitioning and by sulfide extraction, and the decoupled behaviour of Rh is a consequence of the inability of Rh to form its own alloy phase.

4.4. Behaviour of Rh and incongruent melting of sulfides

Rhodium behaves like IPGEs in basalts and picrites, but like Pt and Pd in komatiites. This implies a change in controlling phase, and that this change is related to degree and/or temperature of partial melting. As noted previously, Rh shares with Pd and (under most circumstances) Pt the property that it tends not to form its own phases in mantle samples, but with IPGEs the tendency to partition into MSS during fractionation or incongruent melting of sulfide. The partition coefficients for Pt, Rh and Ir are 0.17, 4.1 and 5.7 respectively, based on data of Barnes et al. (1997). The IPGEs and Rh tend to form extremely strongly correlated arrays within MSS-differentiated orebodies (Barnes, 2004; Li et al., 1992; Mungall, 2007a). Hence, the behaviour of Rh suggests that a critical control may be the presence of solid MSS during mantle melting, and that this may be a consequence of incongruent melting at the lower degrees of partial melting represented by IPGE-Rh depleted basalts.

Bockrath et al. (2004) and subsequently Ballhaus et al. (2006) suggested that incongruent melting of sulfide within the melting range of mantle peridotite can lead to fractionation of the PGEs from one another at source, although Mungall and Brenan (2014) concluded that the overlap between the melting ranges of sulfide and silicate is very limited under most normal mantle melting conditions. Lorand et al. (2012) suggest on the basis of detailed studies of PGE deportment in metasomatised mantle samples that disequilibrium melting of mantle may involve selective retention of MSS inclusions in silicates, while Pt and Pd are released into the melt from accessible interstitial pockets.

The observation that Rh behaves like Pt in komatiites, but like IPGEs in basalts, is consistent with the idea that incongruent sulfide melting with MSS control operates at lower degrees of partial melting. However, incongruent sulfide melting, or any other process such as selective melting of a Pt–Pd enriched "metasomatic sulfide" component (Lorand et al., 2012) is not the dominant control on variance in the mantle sample dataset. Such a process would result in a wide range in Pt/Rh ratios in the mantle residue, particularly at lower degrees of partial melting. This is not consistent with the observation that Pt and Rh correlate strongly across the entire mantle sample data set, and particularly strongly within mantle samples in the upper half of the Al_2O_3 range (Fig. 10), i.e. samples representing either low degrees of melting or high degrees of refertilization.

As shown in the modelling of Mungall and Brenan (2014) based on experimental partition coefficients, Rh has a moderate degree of compatibility in olivine, and this may be sufficient to account for the difference in Pt/Rh between low degree and high degree partial melts. However, olivine control should result in progressive change in Pt/Rh ratio with degree of partial melting in melts formed at a high enough degree of partial melting to exhaust source sulfide. This is not consistent with the observation that Pt, Pd and Rh are correlated in komatiites, but it is consistent with the observation that Pt is depleted relative to Rh in highly melt-depleted cratonic mantle samples. The discrepancy may be explained by temperature dependence on the partitioning of Rh into olivine, but data are lacking to test this at present. The behaviour of Rh therefore remains an enigma. Detailed modelling using the methodology of Mungall and Brenan (2014), combined with a larger set of experimental data on partitioning behaviour of Rh, is required to test incongruent sulfide melting models as well as olivine control.

4.5. Bushveld Complex parent magmas

Bushveld B1 magma patterns are generally similar to those for komatiites except for being distinctly enriched in Pt and Rh and slightly depleted in Ni, Os and Ir (although not Ru). The komatiite-like patterns are consistent with previous interpretations that these magmas are essentially highly contaminated komatiites (Barnes, 1989; Wilson, 2012), and an explanation for the unusually high values of Pt, Pd and Rh may be that these are unusually fractionated and contaminated sulfide-undersaturated magmas derived from komatiite parents with normal contents of these elements. This is advanced as an alternative to the hypothesis that the B1 magmas are derived from exotic, PGE-enriched and highly "fertilized" sub-continental lithospheric mantle, accounting for features such as highly radiogenic Os and Sr and strong enrichment in lithophile trace elements (Richardson and Shirey, 2008). All of these features are also potentially explicable by crustal contamination, but raise considerable difficulties in that extensive crustal contamination should result in dilution of PGE abundances (Barnes et al., 2010), and more rapid depletion of MgO for a given temperature, both of which features are inconsistent with observations. Such an explanation also raises the considerable difficulties of distinguishing geochemical effects of SCLM enrichment from crustal contamination, where both processes involve deep processes and unseen components (Arndt, 2013). Mungall and Brenan (2014) proposed that remelting at high pressure of mantle with high Pt/Pd due to a previous low pressure melting event could produce the unusually high Pt/Pd observed in Bushveld magmas. This controversy is likely to continue and is unlikely to be resolved on PGE data alone; however, the similarity of B1 PGE patterns to komatiite patterns is striking.

5. Conclusions

1 The mantle dataset records a significant variability that can be attributed to highly correlated sampling errors due to the presence of widely varying proportions of a sulfide component with approximately constant PGE proportions.

2 A subset of orogenic peridotite samples has compositions we consider to be representative of the convecting upper mantle, with inter-element PGE ratios strikingly similar to lunar impact breccias, suggesting that both reservoirs owe their PGE endowments to the late meteoritic bombardment.

3 Superimposed on the primordial sulfide component, mantle samples display a PGE signal that records partial melt extraction, in a variety of different melting environments. Off-craton peridotites show extreme depletions in all PGE even at higher Al_2O_3 contents, and oceanic or ophiolitic peridotites tend to show little depletion in any PGE down to very low Al_2O_3.

4 Among the various inter-element correlations in the mantle data set, apart from those between Ru, Ir and Os, the strongest is between Pt and Rh. This is significant because of the tendency of Rh to partition into MSS, like IPGEs but unlike Pt and Pd. This relationship between Pt and Rh limits the significance of MSS control to low degrees of partial melting.

5 Metasomatic processes are evident in a small population of samples with elevated PPGE abundances, but are not a dominant control in the overall variability within the mantle dataset.

6 Mantle melt compositions are PGE undepleted where they form by sufficiently high degrees of partial melting to dissolve all the sulfides in their sources, while otherwise being PGE depleted due to source saturation. The PGE depletions observed in OIBs may result from their derivation from pyroxenitic mantle whose PGE budget has been severely diluted.

7 Many basalt samples have moderate Pt and Pd contents generally taken to imply they have not experienced sulfide saturation, but still have significantly lower Pt and Pd contents than komatiites. This is attributed to pooling and mixing of sulfide-saturated and sulfide-unsaturated partial melts formed at a range of depths.

Please cite this article as: Barnes, S.J., et al., Platinum group elements in mantle melts and mantle samples, Lithos (2015), http://dx.doi.org/10.1016/j.lithos.2015.07.007

8 Basalts with Pt and Pd contents higher than typical komatiites are very rare, with the notable exception of B1-type parent magmas to the Bushveld Complex, which are moderately enriched in Pt and Rh. These have komatiite-like PGE patterns but appear to record some contribution from the high Pt/Pd Kaapvaal lithospheric mantle.

9 The melt complement to the widespread Pd depletion in subcratonic lithosphere is most likely to be MORB, being the only mantle melts with consistently high Pd/Pt. The missing Pd could be sequestered in whatever mantle reservoir presently contains foundered or subducted Archean crust extracted from the subcontinental lithosphere.

Acknowledgments

This manuscript has benefited from extensive discussions over many years with many colleagues, notably Sarah-Jane Barnes, Reid Keays, James Brenan and Ian Campbell. It was improved by preliminary reviews by Reid Keays and Belinda Godel and reviews of the originally submitted version by Edward Ripley and an anonymous reviewer. We thank all the many researchers whose data are included and we apologise that restrictions on the number of references permitted by the journal prevent us from fully citing all data sources in the main text. Full citation details can be found in the supplementary materials. We particularly thank Chris Dale, Hannah Hughes, George Ma and Simon Jowitt for updating partially published data sets. This is a contribution from the CSIRO Mineral Resources Flagship.

Appendix A. Supplementary data

Supplementary data to this article can be found online at http://dx.doi.org/10.1016/j.lithos.2015.07.007.

References

Alard, O., Griffin, W.L., Lorand, J.P., Jackson, S.E., O'Reilly, S.Y., 2000. Non-chondritic distribution of the highly siderophile elements in mantle sulfides. Nature 407, 891–894.

Andrews, D.R.A., Brenan, J.M., 2002a. Phase-equilibrium constraints on the magmatic origin of laurite + Ru–Os–Ir alloy. Canadian Mineralogist 40, 1705–1716.

Andrews, D.R.A., Brenan, J.M., 2002b. The solubility of ruthenium in sulfide liquid; implications for platinum group mineral stability and sulfide melt-silicate melt partitioning. Chemical Geology 192, 163–181.

Arai, S., Prichard, H.M., Matsumoto, I., Fisher, P.C., 1999. Platinum-group minerals in podiform chromitite from the Kamuikotan zone, Hokkaido, northern Japan. Resource Geology 49, 39–47.

Arndt, N.T., 2013. The lithospheric mantle plays no active role in the formation of magmatic ore deposits. Economic Geology 108.

Arndt, N.T., Lesher, C.M., Barnes, S.J., 2008. Komatiite. Cambridge University Press, Cambridge.

Aulbach, S., Mungall, J.E., Pearson, D.G., 2015. Distribution and processing of highly siderophile elements in cratonic mantle lithosphere. Reviews in Geochemistry and Mineralogy — Highly Siderophile and Strongly Chalcophile Elements in High Temperature Geochemistry and Cosmochemistry (in press).

Bai, W.J., Robinson, P.T., Fang, Q.S., Yang, J.S., Yan, B.G., Zhang, Z.M., Hu, X.F., Zhou, M.F., Malpas, J., 2000. The PGE and base-metal alloys in the podiform chromitites of the Luobusa ophiolite, southern Tibet. Canadian Mineralogist 38, 585–598.

Ballhaus, C., Sylvester, P., 2000. Noble metal enrichment processes in the Merensky Reef, Bushveld Complex. Journal of Petrology 41, 545–561.

Ballhaus, C., Bockrath, C., Wohlgemuth-Ueberwasser, C., Laurenz, V., Berndt, J., 2006. Fractionation of the noble metals by physical processes. Contributions to Mineralogy and Petrology 152, 667–684.

Barnes, S.-J., 1985. The petrography and geochemistry of komatiite flows from the Abitibi greenstone belt, and a model for their formation. Lithos 18, 241–270.

Barnes, S.J., 1989. Are Bushveld U-type parent magmas boninites or contaminated komatiites? Contributions to Mineralogy and Petrology 101, 447–457.

Barnes, S.J., 1993. Partitioning of the platinum group elements and gold between silicate and sulfide magmas in the Munni Munni Complex, Western Australia. Geochimica et Cosmochimica Acta 57, 1277–1290.

Barnes, S.J., 2004. Komatiites and nickel sulfide ores of the Black Swan area, Yilgarn Craton, Western Australia. 4. Platinum Group Element distribution in the ores, and genetic implications. Mineral Deposits 39, 752–765.

Barnes, S.J., Fiorentini, M.L., 2008. Iridium, ruthenium and rhodium in komatiites: evidence for iridium alloy saturation. Chemical Geology 257, 44–58.

Barnes, S.-J., Lightfoot, P.C., 2005. Formation of magmatic nickel sulfide deposits and processes affecting their copper and platinum group element contents. Economic Geology 100th Anniversary Volume, 179–214.

Barnes, S.J., Liu, W., 2012. Pt and Pd mobility in hydrothermal fluids: evidence from komatiites and from thermodynamic modelling. Ore Geology Reviews 44, 49–58.

Barnes, S.-J., Picard, C.P., 1993. The behavior of platinum-group elements during partial melting, crystal fractionation, and sulfide segregation: an example from the Cape Smith Fold Belt, Northern Quebec. Geochimica et Cosmochimica Acta 57, 79–87.

Barnes, S.-J., Naldrett, A.J., Gorton, M.P., 1985. The origin of the fractionation of the platinum-group elements in terrestrial magmas. Chemical Geology 53, 303–323.

Barnes, S.-J., Makovicky, E., Makovicky, M., Rose-Hansen, J., Karupmoller, S., 1997. Partition coefficients for Ni, Cu, Pd, Pt, Rh, And Ir between monosulfide solid solution and sulfide liquid and the formation of compositionally zoned Ni–Cu Sulfide bodies by fractional crystallization of sulfide liquid. Canadian Journal of Earth Sciences 34, 366–374.

Barnes, S.-J., Maier, W.D., Ashwal, L.D., 2004a. Platinum-group element distribution in the main zone and upper zone of the Bushveld Complex, South Africa. Chemical Geology 208, 293–317.

Barnes, S.J., Hill, R.E.T., Perring, C.S., Dowling, S.E., 2004b. Lithogeochemical exploration for komatiite-associated Ni-sulfide deposits: strategies and limitations. Mineralogy and Petrology 82, 259–293.

Barnes, S.-J., Prichard, H.M., Cox, R.A., Fisher, P.C., Godel, B., 2008. The location of the chalcophile and siderophile elements in platinum group element ore deposits (a textural, microbeam and whole rock geochemical study); implications for the formation of the deposits. Chemical Geology 248, 295–317.

Barnes, S.-J., Maier, W.D., Curl, E.A., 2010. Composition of the marginal rocks and sills of the Rustenburg Layered Suite, Bushveld Complex, South Africa: implications for the formation of platinum group element deposits. Economic Geology 105, 1491–1512.

Barnes, S.J., Osborne, G.A., Cook, D., Barnes, L., Maier, W.D., Godel, B.M., 2011. The Santa Rita Nickel Sulfide Deposit in the Fazenda Mirabela Intrusion, Bahia, Brazil: geology, sulfide geochemistry and genesis. Economic Geology 106, 1083–1110.

Barnes, S.J., Heggie, G.J., Fiorentini, M.L., 2013. Spatial variation in platinum group element concentrations in ore-bearing komatiite at the Long-Victor deposit, Kambalda Dome, Western Australia: enlarging the footprint of nickel sulfide orebodies. Economic Geology 108, 913–933.

Barnes, S.J., Fisher, L.M., Godel, B., Maier, W.D., Ryan, C.G., Paterson, D., Spiers, K., 2014. Microtextural associations of primary magmatic Pt phases in Pt-rich, S-poor ultramafic cumulates, and implications for the magmatic fractionation of Pt from Pd. 13th International Platinum Symposium. Russian Academy of Sciences, Ural Branch, Yekaterinburg, Russia, pp. 19–20.

Becker, H., Horan, M.F., Walker, R.J., Gao, S., Lorand, J.-P., Rudnick, R.L., 2006. Highly siderophile element composition of the Earth's primitive mantle: constraints from new data on peridotite massifs and xenoliths. Geochimica et Cosmochimica Acta 70, 4528–4550.

Begg, G.C., Hronsky, J.A.M., Arndt, N.T., Griffin, W.L., O'Reilly, S.Y., Hayward, N., 2010. Lithospheric, cratonic and geodynamic setting of Ni–Cu–PGE sulfide deposits. Economic Geology 105, 1057–1070.

Bockrath, C., Ballhaus, C., Holzheid, A., 2004. Fractionation of the platinum-group elements during mantle melting. Science 305, 1951–1953.

Borisov, A.A., 2005. Crystallization and stability of noble metal alloys in the magmatic process. ORE DEPOSITSGeology 47, 469–475.

Borisov, A., Palme, H., 1995. Solubility of iridium in silicate melts: new data from experiments with Ir10Pt90 alloys. Geochimica et Cosmochimica Acta 59, 481–485.

Borisov, A., Palme, H., 2000. Solubilities of noble metals in Fe-containing silicate melts as derived from experiments in Fe-free systems. American Mineralogist 85, 1665–1673.

Botcharnikov, R.E., Holtz, F., Mungall, J.E., Beermann, O., Linnen, R.L., Garbe-Schoenberg, D., 2013. Behavior of gold in a magma at sulfide–sulfate transition; revisited. American Mineralogist 98, 1459–1464.

Brenan, J.M., Andrews, D., 2001. High-temperature stability of laurite and Ru–Os–Ir alloy and their role in PGE fractionation in mafic magmas. Canadian Mineralogist 39, 341–360.

Brenan, J.M., McDonough, W.F., Ash, R., 2003. Experimental constraints on the partitioning of rhenium and some platinum group-elements between olivine and silicate melt. Earth and Planetary Science Letters 212, 135–150.

Brenan, J.M., McDonough, W.F., Ash, R., 2005. An experimental study of the solubility and partitioning of iridium, osmium and gold between olivine and silicate melt. Earth and Planetary Science Letters 237, 855–872.

Brenan, J.M., Finnigan, C.S., McDonough, W.F., Homolova, V., 2012. Experimental constraints on the partitioning of Ru, Rh, Ir, Pt and Pd between chromite and silicate melt; the importance of ferric iron. Chemical Geology 302–303, 16–32.

Brügmann, G.E., Naldrett, A.J., Asif, M., Lightfoot, P.C., Gorbachev, N.S., Fedorenko, V.A., 1993. Siderophile and chalcophile metals as tracers of the evolution of the Siberian Trap in the Noril'sk region, Russia. Geochimica et Cosmochimica Acta 57, 2001–2018.

Campbell, I.H., Barnes, S.J., 1984. A model for the geochemistry of the platinum group elements in magmatic sulfide deposits. Canadian Mineralogist 22, 151–160.

Chou, C., 1978. Fractionation of siderophile elements in the Earth's upper mantle. Proc. 9th Lunar Planet. Science Conference 9, 219–230.

Chu, X.L., Sun, M., Zhou, M.F., 2001. The platinum-group element geochemistry in chemical geodynamics. Acta Petrologica Sinica 17, 112–122.

Chung, H.-Y., Mungall, J.E., 2009. Physical constraints on the migration of immiscible fluids through partially molten silicates, with special reference to magmatic sulfide ores. Earth and Planetary Science Letters 286, 14–22.

Crocket, J.H., 1979. Platinum group elements in mafic and ultramafic rocks: a survey. Canadian Mineralogist 17, 391–403.

Dare, S.A.S., Barnes, S.-J., Prichard, H.M., Fisher, P.C., 2010. The timing and formation of platinum-group minerals from the Creighton Ni–Cu–platinum-group element sulfide deposit, Sudbury, Canada; early crystallization of PGE-rich sulfarsenides. Economic Geology 105, 1071–1096.

Day, J.M.D., Pearson, D.G., Hulbert, L.J., 2013. Highly siderophile element behaviour during flood basalt genesis and evidence for melts from intrusive chromitite formation in the Mackenzie large igneous province. Lithos (Oslo) 182–183, 242–258.

Please cite this article as: Barnes, S.J., et al., Platinum group elements in mantle melts and mantle samples, Lithos (2015), http://dx.doi.org/10.1016/j.lithos.2015.07.007

Distler, V.V., Sluzhenikin, S.F., Cabri, L.J., Krivolutskaya, N.A., Turovtsev, D.M., Golovanova, T.A., Mokhov, A.V., Knauf, V.V., Oleshkevich, O.I., 1999. Platinum ores of the Noril'sk layered intrusions: magmatic and fluid concentration of noble metals. Ore DepositsGeology 41, 214–237.

Ertel, W., O'Neill, H.S.C., Sylvester, P.J., Dingwell, D.B., 1999. Solubilities of Pt and Rh in a haplobasaltic silicate melt at 1300 degrees C. Geochimica et Cosmochimica Acta 63, 2439–2449.

Fabriès, J., Lorand, J.-P., Bodinier, J.-L., 1998. Petrogenetic evolution of orogenic lherzolite massifs in the central and western Pyrenees. Tectonophysics 292, 145–167.

Finnigan, C.S., Brenan, J.M., Mungall, J.E., McDonough, W.F., 2008. Experiments and models bearing on the role of chromite as a collector of platinum group minerals by local reduction. Journal of Petrology 49, 1647–1665.

Fiorentini, M.L., Barnes, S.J., Lesher, C.M., Heggie, G.J., Keays, R.R., Burnham, O.M., 2010. Platinum-group element geochemistry of mineralized and non-mineralized komatiites and basalts. Economic Geology 105, 795–823.

Fischer-Goedde, M., Becker, H., Wombacher, F., 2011. Rhodium, gold and other highly siderophile elements in orogenic peridotites and peridotite xenoliths. Chemical Geology 280, 365.

Fleet, M.E., Stone, W.E., Crocket, J.H., 1991. Partitioning of palladium, iridium and platinum between sulfide liquid and basalt melt: effects of melt composition, concentration and oxygen fugacity. Geochimica et Cosmochimica Acta 55, 2545–2554.

Fonseca, R.O.C., Campbell, I.H., O'Neill, H.S.C., Allen, C.M., 2009. Solubility of Pt in sulfide mattes: implications for the genesis of PGE-rich horizons in layered intrusions. Geochimica et Cosmochimica Acta 73.

Fonseca, R.O.C., Laurenz, V., Mallmann, G., Luguet, A., Hoehne, N., Jochum, K.P., 2012. New constraints on the genesis and long-term stability of Os-rich alloys in the Earth's mantle. Geochimica et Cosmochimica Acta 87, 227.

Gaetani, G.A., Grove, T.L., 1997. Partitioning of moderately siderophile elements among olivine, silicate melt and sulfide melt — constraints on core formation on Earth and Mars Geochim. Cosmochimica Acta 61, 1829–1846.

Garuti, G., Fershtater, G., Bea, F., Montero, P., Pushkarev, E.V., Zaccarini, F., 1997. Platinum-group elements as petrological indicators in mafic-ultramafic complexes of the central and Southern Urals — preliminary results. Tectonophysics 276, 181–194.

Godel, B., Rudashevsky, N.S., Nielsen, T.F.D., Barnes, S.J., Rudashevsky, V.N., 2014. New constraints on the origin of the Skaergaard Intrusion Cu–Pd–Au mineralization: insights from high-resolution X-ray computed tomography. Lithos 190–191, 27–36.

Griffin, W.L., Graham, S., O'Reilly, S.Y., Pearson, N.J., 2004. Lithosphere evolution beneath the Kaapvaal Craton; Re–Os systematics of sulfides in mantle-derived peridotites. Chemical Geology 208, 89.

Griffin, W., O'Reilly, S.Y., Begg, G.C., 2013. Continental-root control on the genesis of magmatic ore deposits. Nature Geoscience 6, 905–910.

Hamlyn, P.R., Keays, R.R., 1986. Sulfur saturation and second stage melts: application to the Bushveld platinum metal deposits. Economic Geology 81, 1431–1445.

Hatton, C.J., Sharpe, M.R., 1989. Significance and Origin of Boninite-like Rocks Associated With the Bushveld Complex. In: Crawford, A.J. (Ed.)Unwin Hyman Inc, London, pp. 174–208.

Helmy, H.M., Ballhaus, C., Fonseca, R.O.C., Wirth, R., Nagel, T., Tredoux, M., 2013. Noble metal nanoclusters and nanoparticles precede mineral formation in magmatic sulfide melts. Nature Communications 4 (article 2405).

Herzberg, C., Asimow, P.D., Arndt, N., Niu, Y., Lesher, C.M., Fitton, J.G., Cheadle, M.J., Saunders, A.D., 2007. Temperatures in ambient mantle and plumes; constraints from basalts, picrites, and komatiites. Geochemistry, Geophysics, Geosystems — G (super 3) 8 (@Q02006).

Hughes, S.R., McDonald, I., Kerr, A.C., 2015. Platinum-group element signatures in the North Atlantic Igneous Province: implications for mantle controls on metal budgets during continental breakup. Lithos (in press) http://dx.doi.org/10.1016/j.lithos.2015.05.005.

Huminicki, M.A.E., Sylvester, P.J., Carbi, L.J., Lesher, C.M., Tubrett, M., 2005. Quantitative mass balance of platinum group elements in the Kelly Lake Ni–Cu–PGE deposit copper cliff offset. Sudbury Economic Geology 100, 1631–1646.

Ireland, T.J., Walker, R.J., Garcia, M.O., 2009. Highly siderophile element and Os-187 isotope systematics of Hawaiian picrites: implications for parental melt composition and source heterogeneity. Chemical Geology 260, 112–128.

Keays, R.R., 1995. The role of komatiitic and picritic magmatism and S-saturation in the formation of ore deposits. Lithos 34, 1–18.

Keays, R.R., Crocket, J.H., 1970. A study of precious metals in Sudbury nickel irruptive ores. Economic Geology 65, 438–450.

Keays, R.R., Davidson, R.M., 1976. Palladium, iridium and gold in the ores and host rocks of nickel sulfide deposits in Western Australia. Economic Geology 71, 214–228.

Keays, R.R., Lightfoot, 2010. Crustal sulfur is required to form magmatic Ni–Cu sulfide deposits; evidence from chalcophile element signatures of Siberian and Deccan Trap basalts. Mineral Deposits 45, 241.

Keays, R.R., Lightfoot, P.C., Hamlyn, P.R., 2012. Sulfide saturation history of the Stillwater Complex, Montana: chemostratigraphic variation in platinum group elements. Mineral Deposits 47, 151–173.

Kennedy, B., Tredoux, M., Ballhaus, C., Coetsee, E., Steyl, G., Anonymous, 2013. Possible PGE nano structures, in magmatic systems. Mineralogical Magazine 77, 1447.

Laurenz, V., Fonseca, R.O.C., Ballhaus, C., Jochum, K.P., Heuser, A., Sylvester, P.J., 2013. The solubility of palladium and ruthenium in picritic melts; 2, the effect of sulfur. Geochimica et Cosmochimica Acta 108, 172–183.

Legendre, O., Auge, T., 1986. Mineralogy of Platinum-group Mineral Inclusions in Chromitites From Different Ophiolitic Complexes. In: Gallagher, M.J., Ixer, R.A., Neary, C.R., Prichard, H.M. (Eds.), Institute of Mining and Metallurgy, London, pp. 361–372.

Lesher, C.M., Burnham, O.M., Keays, R.R., Barnes, S.J., Hulbert, L., 2001. Trace-element geochemistry and petrogenesis of barren and ore-associated komatiites. Canadian Mineralogist 39, 673–696.

Li, C., Naldrett, A.J., Coats, C.J.A., Johannessen, P., 1992. Platinum, palladium, gold and copper-rich stringers at the Strathcona Mine, Sudbury: their enrichment by fractionation of a sulfide liquid. Economic Geology 87, 1584–1598.

Li, C., Barnes, S.-J., Makovicky, E., Rose-Hansen, J., Makovicky, M., 1996. Partitioning of Ni, Cu, Ir, Rh, Pt and Pd between monosulfide solid solution and sulfide liquid: effects of composition and temperature. Geochimica et Cosmochimica Acta 60, 1231–1238.

Li, J., Xu, J.F., Suzuki, K., He, B., Xu, Y.G., Ren, Z.Y., 2010. Os, Nd and Sr isotope and trace element geochemistry of the Muli picrites: insights into the mantle source of the Emeishan Large Igneous Province. Lithos 119, 108–122.

Li, C., Tao, Y., Qi, L., Ripley, E.M., 2012. Controls on PGE fractionation in the Emeishan picrites and basalts; constraints from integrated lithophile–siderophile elements and Sr–Nd isotopes. Geochimica et Cosmochimica Acta 90, 12.

Lightfoot, P.C., Keays, R.R., 2005. Siderophile and chalcophile metal variations in flood basalts from the Siberian Trap, Noril'sk Region: implications for the origin of the Ni–Cu–PGE sulfide ores. Economic Geology 100, 439–462.

Lightfoot, P.C., Naldrett, A.J., Gorbachev, N.S., Fedorenko, V.A., Hawkesworth, C.J., Hergt, J., Doherty, W., 1992. Chemostratigraphy of Siberian Trap Lavas, Noril'sk District: Implications for the Source of Flood Basalt Magmas and Their Associated Ni–Cu Mineralization. In: Lightfoot, P.C., Naldrett, A.J. (Eds.), Ontario Geological Survey, Toronto, pp. 283–312.

Liipo, J., 1999. Platinum-group minerals from the Paleoproterozoic chromitite, Outokumpu ophiolite complex, eastern Finland. Ofioliti 24, 217–222.

Locmelis, M., Pearson, N.J., Barnes, S.J., Fiorentini, M.L., 2011. Ruthenium in komatiitic chromite. Geochimica et Cosmochimica Acta 75, 3645–3661.

Lorand, J.-P., Alard, O., Godard, M., 2008a. Platinum-group element signature of the primitive mantle rejuvenated by melt-rock reactions: evidence from Sumail peridotites (Oman Ophiolite). Terra Nova 21, 35–40.

Lorand, J.-P., Luguet, A., Alard, O., 2008b. Platinum-group elements; a new set of key tracers for the Earth's interior. Elements 4, 247–252.

Lorand, J.-P., Luguet, A., Alard, O., Bezos, A., Meisel, T., 2008c. Abundance and distribution of platinum-group elements in orogenic lherzolites; a case study in A Fontete Rouge Lherzolite (French Pyrenees). Chemical Geology 248, 174–194.

Lorand, J.P., Alard, O., Luguet, A., 2010. Platinum-group element micronuggets and refertilization process in Lherz orogenic peridotite (northeastern Pyrenees, France). Earth and Planetary Science Letters 289, 298–310.

Lorand, J.-P., Luguet, A., Alard, O., 2012. Platinum-group element systematics and petrogenetic processing of the continental upper mantle: a review. Lithos 164, 2–21.

Luguet, A., Lorand, J.P., Seyler, M., 2003. Sulfide petrology and highly siderophile element geochemistry of abyssal peridotites: a coupled study of samples from the Kane Fracture Zone (45 degrees W 23 degrees 20N, MARK Area, Atlantic Ocean). Geochimica et Cosmochimica Acta 67, 1553–1570.

Luguet, A., Shirey, S.B., Lorand, J.-P., Horan, M.F., Carlson, R.W., 2007a. Residual platinum-group minerals from highly depleted harzburgites of the Lherz Massif (France) and their role in HSE fractionation of the mantle. Geochimica et Cosmochimica Acta 71, 3082.

Luguet, A., Shirey, S.B., Lorand, J.P., Horan, M.F., Carlson, R.W., 2007b. Residual platinum-group minerals from highly depleted harzburgites of the Lherz Massif (France) and their role in HSE fractionation of the mantle. Geochimica et Cosmochimica Acta 71, 3082–3097.

Ma, G.S.K., Malpas, J., Gao, J., Wang, K.-L., Qi, L., Xenophontos, C., 2013. Platinum group element geochemistry of intraplate basalts from the Aleppo Plateau, NW Syria. Geological Magazine 150, 497–508.

Maier, W.D., Barnes, S.J., 1999. Platinum-group elements in silicate rocks of the Lower, Critical and Main Zones at union section, western Bushveld Complex. Journal of Petrology 40, 1647–1671.

Maier, W.D., Barnes, S.J., de Klerk, W.J., Teigler, B., Mitchell, A.A., 1996. Cu/Pd and Cu/Pt of silicate rocks in the Bushveld Complex; implications for platinum-group element exploration. Economic Geology 91, 1151–1158.

Maier, W.D., Barnes, S.J., Campbell, I.H., Fiorentini, M.L., Peltonen, P., Barnes, S.-J., Smithies, R.H., 2009. Progressive mixing of meteoritic veneer into the early Earth's deep mantle. Nature 460, 620–623.

Maier, W.D., Peltonen, P., McDonald, I., Barnes, S.J., Barnes, S.-J., Hatton, C., Viljoen, F., 2012. The concentration of platinum-group elements and gold in southern African and Karelian kimberlite-hosted mantle xenoliths: implications for the noble metal content of the Earth's mantle. Chemical Geology 302–303, 119–135.

Maier, W.D., Rasmussen, B., Fletcher, I., Godel, B., Barnes, S.J., Fisher, L., Yang, S.H., Huhma, H., Lahaye, Y., 2015. Petrogenesis of the ~2.77 Ga Monts de Cristal Complex, Gabon: evidence for direct precipitation of Pt-arsenides from basaltic magma. Journal of Petrology (in press).

Malitch, K.N., Thalhammer, O.A.R., 2002. Pt–Fe nuggets derived from clinopyroxenite–dunite massifs, Russia: a structural, compositional and osmium-isotope study. Canadian Mineralogist 40, 395–418.

Mavrogenes, J.A., O'Neill, H.S.C., 1999. The relative effects of pressure, temperature and oxygen fugacity on the solubility of sulfide in mafic magmas. Geochimica et Cosmochimica Acta 63, 1173–1180.

McDonough, W.F., Sun, S.-S., 1995. The composition of the Earth. Chemical Geology 120, 223–253.

McInnes, B.I.A., McBride, J.S., Evans, N.J., Lambert, D.D., Andrew, A.S., 1999. Osmium isotope constraints on ore metal recycling in subduction zones. Science 286, 512–516.

Momme, P., Tegner, C., Brooks, C.K., Keays, R.R., 2002. The behaviour of platinum-group elements in basalts from the East Greenland rifted margin. Contributions to Mineralogy and Petrology 143, 133–153.

Please cite this article as: Barnes, S.J., et al., Platinum group elements in mantle melts and mantle samples, Lithos (2015), http://dx.doi.org/10.1016/j.lithos.2015.07.007

Momme, P., Tegner, C., Brooks, C.K., Keays, R.R., 2006. Two melting regimes during Paleogene flood basalt generation in East Greenland: combined REE and PGE modelling. Contributions to Mineralogy and Petrology 151, 88–100.

Morgan, J.W., Walker, R.J., Brandon, A.D., Horan, M.F., 2001. Siderophile elements in Earth's upper mantle and lunar breccias: data synthesis suggests manifestations of the same late influx. Meteoritics and Planetary Science 36, 1257–1275.

Mungall, J.E., 2002. Roasting the mantle: slab melting and the genesis of major Au and Au-rich Cu deposits. Geology 30, 905–918.

Mungall, J.E., 2007. Crystallization of magmatic sulfides; an empirical model and application to Sudbury ores. Geochimica et Cosmochimica Acta 71, 2809.

Mungall, J.E., 2014. 13.8 — geochemistry of magmatic ore deposits. In: Holland, H.D., Turekian, K.K. (Eds.), Treatise on Geochemistry, second edition Elsevier, Oxford, pp. 195–218.

Mungall, J.E., Brenan, J.M., 2014. Partitioning of platinum-group elements and Au between sulfide liquid and basalt and the origins of mantle–crust fractionation of the chalcophile elements. Geochimica et Cosmochimica Acta 125, 265–289.

Mungall, J.E., Andrews, D.R.A., Cabri, L.J., Sylvester, P.J., Tubrett, M., 2005. Partitioning of Cu, Ni, Au, and platinum-group elements between monosulfide solid solution and sulfide melt under controlled oxygen and sulfur fugacities. Geochimica et Cosmochimica Acta 69, 4349.

Mungall, J.E., Hanley, J.J., Arndt, N.T., Debecdelievre, A., 2006. Evidence from meimechites and other low-degree mantle melts for redox controls on mantle–crust fractionation of platinum-group elements. Proceedings of the National Academy of Sciences 103, 12695–12700.

Murthy, V.R., Karato, S., 1997. Core formation and chemical equilibrium in the earth.2. Chemical consequences for the mantle and core. Phys. Earth Planet Interiors 100, 81–95.

Naldrett, A.J., 2004. Magmatic Sulfide Deposits: Geology, Geochemistry and Exploration. Springer, Heidelberg.

Naldrett, A.J., Innes, D.G., Sowa, J., Gorton, M.P., 1982. Compositional variations within and between five Sudbury ore deposits. Economic Geology 77, 1519–1534.

Naldrett, A.J., Lightfoot, P.C., Fedorenko, V., Doherty, W., Gorbachev, N.S., 1992. Geology and geochemistry of intrusions and flood basalts of the Noril'sk region, USSR, with implications for the origin of the Ni–Cu ores. Economic Geology 87, 975–1004.

Naldrett, A.J., Asif, M., Schandl, E., Searcy, T., Morrison, G.G., Binney, W.P., Moore, C., 1999. Platinum-group elements in the Sudbury ores: significance with respect to the origin of different ore zones and to the exploration for footwall orebodies. Economic Geology 94, 185–210.

Norman, M.D., Bennett, V.C., Ryder, G., 2002. Targeting the impactors: siderophile element signatures of lunar impact melts from Serenitatis. Earth and Planetary Science Letters 202, 217–228.

O'Neill, H.S.C., Dingwell, D., Borisov, A., Spettel, B., Palme, H., 1995. Experimental petrochemistry of some highly siderophile elements at high temperatures, and some implications for core formation and the mantle's early history. Chemical Geology 120, 255–273.

Page, N.J., Talkington, R.W., 1984. Palladium, platinum, rhodium, ruthenium and iridium in peridotites from ophiolite complexes in Newfoundland. Canadian Mineralogist 22, 137–149.

Page, P., Barnes, S.-J., Bedard, J.H., Zientek, M.L., 2012. In situ determination of Os, Ir, and Ru in chromites formed from komatiite, tholeiite and boninite magmas; implications for chromite control of Os, Ir and Ru during partial melting and crystal fractionation. Chemical Geology 302–303, 3–15.

Park, J.-W., Campbell, 2013. Platinum alloy and sulfur saturation in an arc-related basalt to rhyolite suite; evidence from the Pual Ridge lavas, the eastern Manus Basin. Geochimica et Cosmochimica Acta 101, 76.

Pattou, L., Lorand, J.P., Gros, M., 1996. Non-chondritic platinum-group element ratios in the Earth's mantle. Nature 379, 712.

Peck, D.C., Keays, R.R., 1990. Geology, geochemistry, and origin of platinum-group element-chromitite occurrences in the Heazlewood River Complex, Tasmania. Economic Geology 85, 765.

Peck, D.C., Keays, R.R., 1992. Direct crystallization of refractory platinum-group element alloys from boninitic magmas; evidence from western Tasmania. Australian Journal of Earth Sciences 39, 373.

Prichard, H.M., Potts, P.J., Neary, C.R., 1981. Platinum group element minerals in the Unst chromite, Shetland Isles. Transactions of the Institution of Mining and Metallurgy Section B 90, 186–188.

Puchtel, I.S., Humayun, M., Campbell, A.J., Sproule, R.A., Lesher, C.M., 2004. Platinum group element geochemistry of komatiites from the Alexo and Pyke Hill areas, Ontario, Canada. Geochimica et Cosmochimica Acta 68, 1361–1383.

Qi, L., Wang, C.Y., Zhou, M.F., 2008. Controls on the PGE distribution of Permian Emeishan alkaline and peralkaline volcanic rocks in Longzhoushan, Sichuan Province, SW China. Lithos 106, 222–236.

Rehkämper, M., Halliday, A.N., Fitton, J.G., Lee, D.C., Wieneke, M., Arndt, N.T., 1999. Ir, Ru, Pt, and Pd in basalts and komatiites: new constraints for the geochemical behavior of the platinum-group elements in the mantle. Geochimica et Cosmochimica Acta 63, 3915–3934.

Richardson, S.H., Shirey, S.B., 2008. Continental mantle signature of Bushveld magmas and coeval diamonds. Nature 453, 910–913.

Roeder, P.L., Emslie, R.F., 1970. Olivine-liquid equilibrium. Contributions to Mineralogy and Petrology 29, 275–282.

Salters, V.J.M., Stracke, A., 2004. Composition of the depleted mantle. Geochemistry, Geophysics, Geosystems 5. http://dx.doi.org/10.1029/2003GC000597.

Seitz, H.M., Keays, R.R., 1997. Platinum group element segregation and mineralization in a noritic ring complex formed from Proterozoic siliceous high magnesium basalt magmas in the Vestfold Hills, Antarctica. Journal of Petrology 38, 703–725.

Sen, P.B., 1968. Estimates of the regression coefficient based on Kendall's Tau. Journal of the American Statistical Association 63, 1379–1389.

Shirey, S.B., Walker, R.J., 1998. The Re–Os isotope system in cosmochemistry and high-temperature geochemistry. Annual Review of Earth and Planetary Sciences 26, 423–500.

Sobolev, A.V., Hofmann, A.W., Sobolev, S.V., Nikogosian, I.K., 2005. An olivine-free mantle source of Hawaiian shield basalts. Nature 434, 590.

Sobolev, A., Hoffman, A., Kuzmin, D., Yaxley, G., Arndt, N., Chung, S.-L., Danyushevsky, L., Elliott, T., Frey, F., Garcia, M., Gurenko, A., Kamenetsky, V., Kerr, A., Krivolutskaya, N., Matvienkov, V., Nikogosian, I., Rocholl, A., Sigurdson, I., Sushchevskaya, N., Teklay, M., 2007. The amount of recycled crust in sources of mantle-derived melts. Science 316, 412–417.

Song, X., Zhou, M., Keays, R., Cao, Z., Sun, M., Qi, L., 2006. Geochemistry of the Emeishan flood basalts at Yangliuping, Sichuan, Sw China: implications for sulfide segregation. Contributions to Mineralogy and Petrology 152, 53–74.

Stanley, C.R., 2003. Estimating sampling errors for major and trace elements in geological materials using a propagation of variance approach. Geochemistry: Exploration, Environment, Analysis 3, 169–178.

Tredoux, M., Lindsay, N.M., Davies, G., McDonald, I., 1995. The fractionation of platinum-group elements in magmatic systems, with the suggestion of a novel causal mechanism. South African Journal of Geology 98, 157–167.

Vogel, D.C., Keays, R.R., 1997. The petrogenesis and platinum-group element geochemistry of the Newer Volcanic Province, Victoria, Australia. Chemical Geology 136, 181–204.

Walter, M.J., 1998. Melting of garnet peridotite and the origin of komatiite and depleted lithosphere. Journal of Petrology 39, 29–60.

Wilson, A.H., 2012. A chill sequence to the Bushveld Complex; insight into the first stage of emplacement and implications for the parental magmas. Journal of Petrology 53, 1123–1168.

Wilson, A.H., Tredoux, M., 1990. Lateral and vertical distribution of platinum-group elements and petrogenetic controls on the sulfide mineralization in the P1 pyroxenite layer of the Darwendale Subchamber of the Great Dyke, Zimbabwe. Economic Geology 85, 556–584.

Zhang, M., O'Reilly, S., Wang, K.-L., Hronsky, J., Griffin, W., 2008. Flood basalts and metallogeny: the lithosphere mantle connection. Earth-Science Reviews 86, 145–174.

Zhou, M.F., Yumul, G.P., Malpas, J., Sun, M., 2000. Comparative study of platinum-group elements in the Coto and Acoje blocks of the Zambales Ophiolite Complex, Philippines. Island Arc 9, 556–564.

Please cite this article as: Barnes, S.J., et al., Platinum group elements in mantle melts and mantle samples, Lithos (2015), http://dx.doi.org/10.1016/j.lithos.2015.07.007